UNIVERSITY OF
EASTERN FINLAND

CHALCONE-BASED CHROMOPHORES FUNCTIONALIZED WITH PHOSPHORUS ELECTRON ACCEPTORS

MASTER'S THESIS

Inorganic Chemistry

International Master's Program for Research Chemists

647/2020

Chalcone-based chromophores functionalized with phosphorus electron acceptors

University of Eastern Finland, Department of Chemistry
Supervisor: Professor, Igor Koshevoy
Joensuu 30.4.2020

Abstract:

The intramolecular charge-transfer (ICT) process occurs within a conjugated molecule from an electron-rich part to the electron-poor part, resulting in different absorption and emission properties, which is shown to be important to biology, like fluorescence sensing and bioimaging, optoelectronic materials and other technological applications. Studies focus on the incorporation of different elements or groups into special conjugated systems to design a specific structure to achieve a certain function or emit a certain color. For example, main group elements were widely studied, such as nitro groups, cyano groups, sulfur-containing groups, boron groups as well as phosphorus-containing groups. Through introducing different electron-donor and electron-acceptor to various π-fragments, electron movement can be tuned by their various electron-pushing and -pulling abilities, leading to the changes on their photophysical properties when combined with a π-spacer.

After the construction of their structures, the photophysical applications and properties were studied, including sensing and response to certain chemicals, pH, polarity, solvatochromism, imaging. Various phosphine oxides attached to different π-spacers have been investigated. Electron-withdrawing abilities of phosphine oxides and phosphonium units promote electron transport, while my work is dedicated to the synthesis and analysis of chalcone-based chromophores functionalized with phosphonium and phosphine oxide acceptors.

The series of phosphonium salts and phosphine oxides were obtained using a variable spacer, one compound was characterized by single-crystal diffraction study. The photophysical properties, including absorption, emission in solutions and in solid state, and some solvent effects were analyzed. Comparison of the length of the conjugation of compounds with the same donors and acceptors was carried out; absorption shape, intensity and the nature of counterions. The variation of acceptors was correlated with the photophysical properties. Furthermore, the influence of solvent polarity was evaluated in chloroform and acetonitrile, and the effect of acidity has also been proved to be governing factors of the ICT process.

Keywords: ICT, Phosphonium salts, Phosphine oxides, Crystal structure, Photophysical properties.

Contents

Abbreviations

NMR	Nuclear magnetic resonance
MS	Mass spectra
XRD	X-ray diffraction
ICT	Intramolecular charge transfer
CN	Cyanide anion
NLO	Nonlinear optics
NIR	Near-infrared
HOMO	Highest occupied molecular orbital
LUMO	Lowest unoccupied molecular orbital
PES	Potential energy surface
KBr	Potassium bromide
PPh_3	Triphenyl phosphine
t-Bu	Tertiary butyl
OPVs	Organic photovoltaic cells
DSSCs	Dye-sensitized solar cells
OLEDs	Organic light-emitting diodes
AIEE	Aggregate-induced enhanced emission
TADF	Thermally activated delayed fluorescence
EQE	External quantum yield
THF	Tetrahydrofuran
DBT	Dibenzothiophene
OPVs	Organic photovoltaic cells
SMOSCs	Single material organic solar cells
PCE	Power conversion efficiency
STED	Stimulated emission depletion

1. An Introduction to the Charge-transfer Process

The phenomenon of excited-state charge-transfer (CT) is of fundamental importance for many fields dealing with photophysical and photochemical properties, starting from biology (photosynthesis and metabolism)[1–3] to modern technological applications, including optoelectronic materials for organic light-emitting diodes (OLEDs), solar energy conversion and nonlinear optics (NLO), fluorescence sensing and bioimaging.[4–6] The transfer of charge typically is an intrinsic feature of organic donor-acceptor (D-A) molecules. When this process occurs within one molecule, charges move from an electron-rich motif (donor) to an electron-poor motif (acceptor), it is termed as intramolecular charge transfer (ICT). This charge transfer generally proceeds in the electronically excited state. In other words, when a molecule interacts with the light of a proper wavelength, the energy absorbed from light can push the electron from one part of a molecule or an ion in the ground state to its other part in the excited state, so it makes a huge change in the charge distribution between the ground and excited states. The through-bond ICT process occurs in a special molecule where a π-conjugated bridge connects the donor and the acceptor groups (Figure 1). In some uncommon cases, the ICT can happen through space when the donor and acceptor groups are in a spatially favorable position (e.g. close proximity).[7]

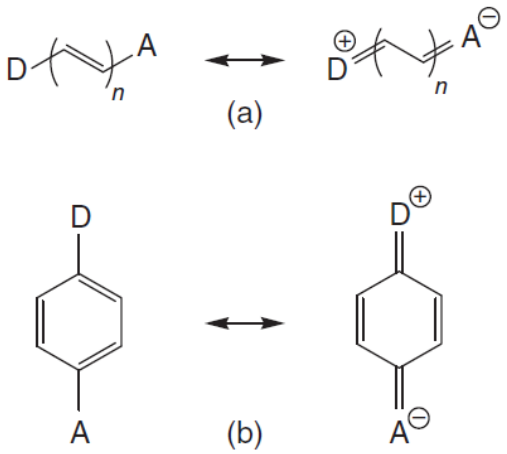

Figure 1 *The illustrations of intramolecular charge-transfer processes in two systems (a) (poly)ene system and (b) aromatic system.*[8]

The π-electron bridge is called chromophore, which can absorb the energy of light of a proper wavelength. Donors and acceptors (auxochromes) are functional groups, which can be viewed as extended conjugated systems by resonance. When they are attached to a chromophore, both the intensity of absorption is altered and the shifted wavelength of UV or visible light is absorbed. Hence the molecule appears colored. When auxochromes are attached to the molecule, the electronic structure of the chromophore gets changed and thus its color is modified.

Examples of donor motifs include: the hydroxyl/alkoxyl group (-OH/-OR), the amino group (-NR_2); the popular acceptors are the nitro group (-NO_2), the cyano group (-CN), the carbonyl group (> C=O) and the phosphorus-containing groups (-PR_2=O/-$PR3^+$). When those auxochromes are connected to a π-fragment, the donor provides more electrons into the conjugated system and enhances the mobility of the electrons. The donor and acceptor change the energy difference between the highest occupied molecular orbital (HOMO) and lowest unoccupied molecular orbital (LUMO), resulting in a verified wavelength.

When light passes through the compound, energy can be absorbed from the light to promote electrons to anti-bonding orbitals from a non-bonding or bonding orbital. The possible electronic transitions are shown in Figure 2.

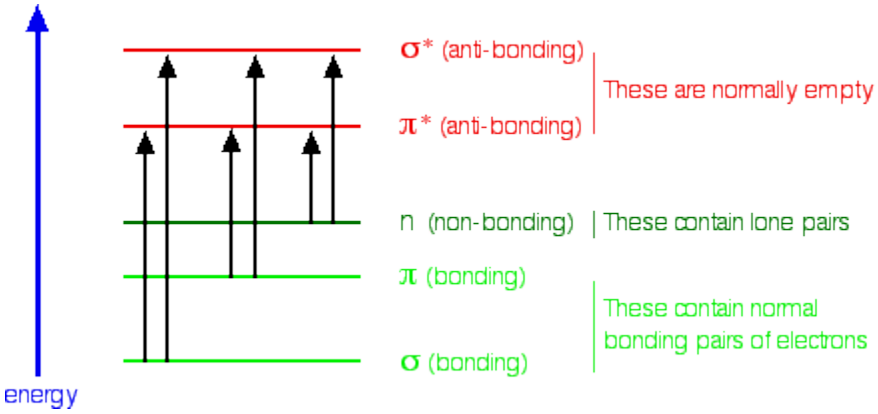

Figure 2 *The demonstration of bonding, non-bonding and anti-bonding energies.*[9]

A filled orbital electron can be excited into an empty anti-bonding orbital when the energy is absorbed from the light. The larger energy gap shown above, the more energy needed, the shorter wavelength absorbed, because every wavelength of light corresponds to certain energy. A photon will be absorbed when the energy of the light is right for the transition gap, promoting an electron to anti-bonding orbitals. The spin of the electron is still paired with the ground-state electron. In the excited state, electrons only stay for a short period of time (ca. 10^{-15} s) and then immediately fall back down into the ground state. Then electrons reach the lowest vibrational level (ν_0) in a form of non-radiative relaxation. Finally, electrons return to the ground state, which can lead to an emission of photons possessing a certain wavelength. When electrons are back to the lowest vibrational level, some energy is lost through vibrational relaxation or dissipation and solvent reorganization, which means the energy of emitted light is lower than that of absorbed light. The difference between wavelength of absorption and emission band maxima is called Stokes shift.

The peaks in emission spectra are at the blue end, which generally comes from a locally excited (LE) state, while the peaks at the red end of its emission spectrum are commonly believed to be ICT process that results in its fluorescence emission sensitive to

environment and solvent polarity.[10–13] Solvent stabilization of molecular excited state also cause stokes-shifted ICT fluorescence.[14]

In Figure 3, the energy of ground state (S_0) and of the two lowest excited states (S_1, S_2) were drawn on potential energy surfaces (PES) as well as the LE and ICT states. The energy of different energy level is represented by vertical coordinate, LE→ICT reaction changes, like bond lengths and angles, are represented by horizontal coordinate (ξ). Excitation of electrons from a molecule can reach S_2 state, then relaxes to equilibrated LE state by internal conversion (vibrations and rotations). In order to achieve LE to the ICT transition, enthalpy difference ΔH and reaction barrier Ea must be overcome. This can give rise to dual luminescence with different emission maxima, $\tilde{\nu}_{max}$ (LE) and $\tilde{\nu}_{max}$ (ICT), respectively, if the transition to the ICT state is incomplete.

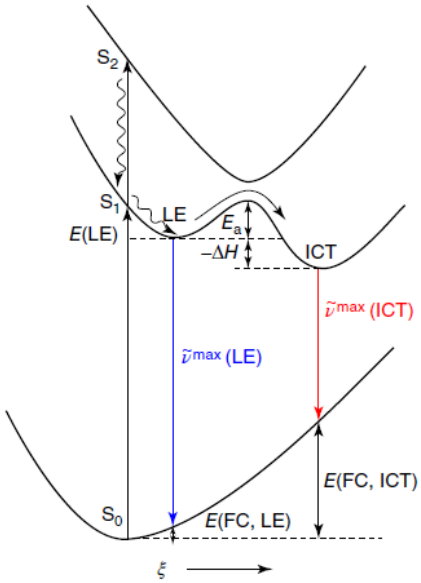

Figure 3 *Schematic representation of ICT process in a model system.*

The S_2 excited state can be reached by exciting a molecule, then through internal conversion, S_1-LE state could be reached. The ICT state can be accessible through the S_1-LE state. Dual emission can occur from LE and ICT emissions of a molecule.[15]

An electron-rich donor is the place where HOMO is localized in D-π-A systems, while an electron-deficient acceptor is a place where LUMO is localized. Donor and acceptor provide lone pairs and orbitals, respectively. The spatial separation of HOMO and LUMO, caused by the conjugated system, causes a formation of special excited states, which are polar because of separated charges. Some factors can also affect ICT processes, such as solvatochromism. Finally, a variation of color can be realized by incorporating different donors and acceptors.

1.1. Solvatochromism

Absorbance/fluorescence spectral properties are strongly affected by solvent effects, like polarity and polarizability of solvents. Due to the ICT, organic compounds could have a greater dipole moment value in their singlet excited state than its ground state.

In order to get a quantitative estimation of solvatochromic parameters, Moyon and Mitra conducted a series of analyses on solvent polarizability and the ability of the solvent to be a hydrogen-bonding donor and a hydrogen-bonding acceptor.[16] Different pure solvents were chosen, they are different in polarity and the ability on hydrogen-bond donating and accepting to figure out their relative contribution to LC solvatochromism. Their analysis unmasks that behavior of lumichrome is influenced by solvent acidity that is an important parameter on characterizing the excited-state. More specifically, redshift was shown in absorption/emission maxima as well as an increase on quantum yield. In a polar protic medium, it is more stable for fluorescence states than in aprotic environments.

The interaction between amphiprotic solvents and a solute molecule, like alcohol, water, and so on, is a contributing factor to the solubility and has impacts on solute chemical properties. New molecular complexes can be formed by hydrogen bonds because of the interactions of amphiprotic solvents and heterocyclic organic compounds. Hydrogen-bonded complex can affect the chemical natures of solutes. The formation of hydrogen bond relays on the special structure of both the solute and solvent. If there are multiple hydrogen bonding positions in one solute molecule, and solvent works as a proton donor and a proton acceptor like acetic acid and water, the situation can become more complicated. Hydrogen bonding interactions among solvent molecules and solute remain inevitable. Besides, the formation of hydrogen bonds in the excited state and tautomerization could be changed due to the redistribution of charges after excitation.

From non-polar solvent to polar solvent, solvent polarity increases, absorbance and fluorescence spectra show an obvious redshift, which implies a stabilized excited state compared to ground state. The charge distribution is reached because of the interaction of the polar solvent and excited state of the solute. A highly stable excited state is formed and longer wavelength of light is released

1.2. Variation of Color

The preparation of long emission-wavelength organic materials and high yield on fluorescence quantum is highly attractive. The charge-transfer process can be achieved through a small polar solvent bandgap by connecting electron-donating and accepting groups to a fluorophore to form D-A scheme, therefore, longer wavelength was emitted. Color variation from blue to red can be tuned by changing different groups. For example,

a cross-coupling reaction catalyzed by nickel (Figure 4)[17] was designed to connect electron donor (1,3,5-triaryl-2-pyrazoline) and an electron acceptor (o-Carborane moiety), redshift (λ_{max} = 596-638 nm) from photoluminescence spectra was observed as well as color-tuning in its solid state, changing from yellow to bright red with good quantum yield (35.7%).

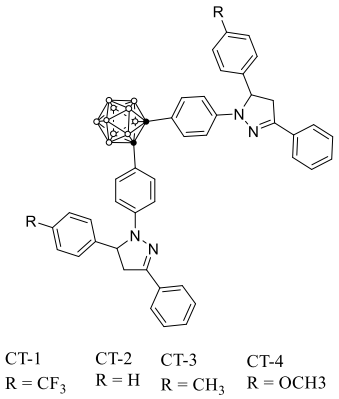

Figure 4 *The structure of o-Carborane-Bis(1,3,5-triaryl-2-pyrazoline) Triads.*[17]

Two most-preferred color Red and NIR are widely applied in fluorescent probes, immune-staining, immunohistochemistry, and biochemistry for optical imaging and analytical sensing.[18] For example, green and red dyes with excitable chromophores are used in the research of tissues and cells without damage after the cells were irradiated with the visible light.

Numerous studies have been conducted in order to construct more complicated fluorescent probes and to explore their specific applications and properties.[19] Fluorescent probes are known by its excellent ability to modulate the optical properties, including excitation and emission spectra, lifetime, intensity, specificity and sensitivity. Most commonly applied biological sensing probes[20] are rhodamine and fluorescein dyes. They have high fluorescence quantum yields, high extinction coefficients and long excitation wavelength ($\lambda \approx 500$ nm). Specific to particular chromophores, donors and acceptors can tune the energy gap between HOMO and LUMO, which can facilitate the design of better fluorescent probes with different color.

2. Main group element acceptors

Tuning the energies of HOMO and LUMO levels can be done by choosing suitable donor and acceptor groups, which can tune absorption energies and can change emission colors.

A conjugated system has been incorporated with donor and acceptor groups for the purpose of tuning the optoelectronic properties to reach the aim of a longer wavelength of fluorescence. But the ability of the electron-pull ability of different acceptor groups

is different. Typical thiadiazoles, diimides, quinoxalines and oxadiazoles are commonly used as acceptors with intermediate electron-withdrawing ability. While nitro moiety is found strong in its excited state, resulting in a more highly polar state and charge transfer state[21] which means that a highly tunable ICT process can be designed by introducing a stronger electron-withdrawing group. Phosphorus centers were also incorporated into organic compounds and electron mobility of guest materials is strengthened.

The P=O bond of the phosphine oxide is very polar. If this electron-withdrawing P=O unit is connected to a conjugated bridge, it can make the connected core electron-deficient and thus improve its electron-transport properties. Therefore, the degree of π-conjugation can be tuned, ability on electron-accepting, solid state packing, the thermal stability of the phosphole materials can also be modified. Organophosphorus-based material is scientifically important and can be applied in dye-sensitized solar cells (DSSCs), organic photovoltaic cells (OPV cells) and organic light-emitting diodes (OLEDs).[22]

The addition of phosphorus-containing acceptor to the conjugated groups can contribute to tune charge transfer and also help in shifting the emission wavelengths further into the red region. Developing a variety of molecules and materials bearing variable electronic properties.

2.1. Nitro group

Through regulating the charge distribution over the molecule, a controllable ICT process can be achieved, suitable acceptor like nitro group groups is the key. -NO_2 group is known as having a strong electron-withdrawing ability, which is expected to disperse electrons on the resonance structure. Besides, the nitro group increases the extent of the expansion of positive potential by attracting electronic charge from conjugated systems. If a conjugated system attaches a strong electron-withdrawing group, the electron distribution can be changed by electron movement from donors. Thus, spectral properties were changed significantly. Nitrophenolate ion and nitro phenolic derivatives have shown significant changes in spectral maxima and pattern of absorption spectra compared to complex that was formed with different amino groups in solution. Until now, few experimental and theoretical studies have been reported related to nitrophenolate derivatives.[23] El-Dossoki has disclosed the ion-pair association of potassium and sodium picrate in 2-butanone by spectroscopic and conductometric analysis.[24]

Panja and co-workers synthesized and studied three nitrophenolate salts with simple substitution with nitro group in ortho and para position (Figure 5). By simply incorporating of nitro groups in the aromatic ring at two different ortho and para positions, two different charge transfer was observed. ICT and $\pi \rightarrow \pi^*$ transition

processes are determined in these derivatives by theoretical calculation and UV-Vis spectroscopy.

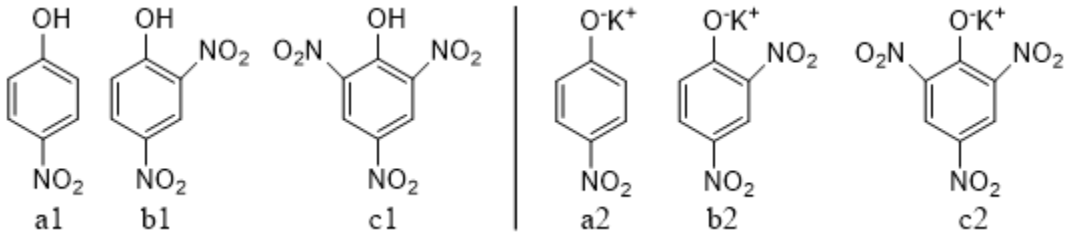

Figure 5 *Nitrophenolate salts with nitro groups in ortho and para position.*[25]

The nitrophenolates serve as D-π-A molecules, upon photoexcitation, an electron from the negatively charged phenolate is transferred to the nitro group, leading to evident charge redistribution among the molecule. The negative charge was dispersed along the benzene ring because of the stronger electron-donating abilities of O^-. As a result, the phenol and the related phenolate ions show distinct absorption optical properties.

2.2. Cyano group

Apart from nitro group, electron-withdrawing cyano groups were incorporated into a conjugated system to achieve intense near-UV emission. The incorporation of cyano groups benefits a lot of molecular materials, which have been reported.[26] For instance, Thomas et al. investigated carbazoles (Figure 6) that can exhibit green emission and enhance its electroluminescence performance functionalized with the incorporation of a cyano group leading to improved enhancement in electron movement;[28] Wong and co-workers discovered an improved electron transport and injection and thermal morphological stability from N,Ndicarbazolyl-3,5-benzene with a cyano group attached with no change of the triplet energy for the functionalization.[29] Incorporation of electron-withdrawing substituent CN affects the emission, thermal, and electronic properties of compounds. Reasonable alteration both in HOMO and in luminescence maximum can be realized by a slight modification of the structure. Specific chromophores, attached with cyano-functionalized carbazole units and connected by acetylene spacer, was chosen.[30] It can behave like an acceptor to regulate the electron-donating strength of the π system of carbazole unit.[31]

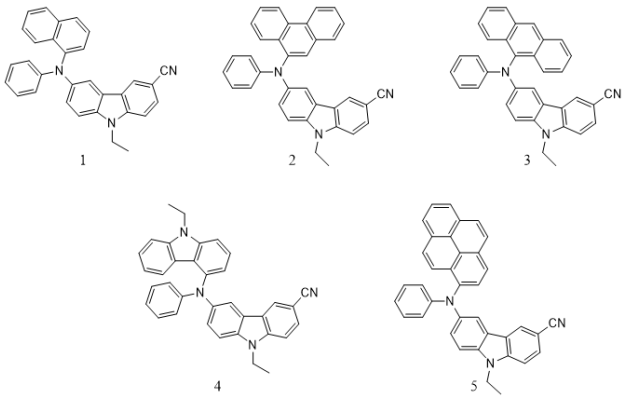

Figure 6 *Carbazoles with a cyano group at C-3 and an arylamine group at C-6.*[28]

While for some compounds, their behaviors in the aggregated state like nanoparticles and crystals or in dilute solution, are different because of several reasons: (1) Internal molecular motion caused nonradiative decay; (2) In aggregated state, rather rigid environment for molecules suppress the nonradiative decay process. Hence the fluorescent behavior shows differences both in the aggregated state and in solution.[32–35] Some fluorescent dyes emit differently when dissolved in solution and in its solid state, strongly emitted in solution but only slightly or no emission in its solid state. While aggregated-state dyes can show higher fluorescence quantum yields than that in dilute solution, which is known as aggregate-induced enhanced emission (AIEE).[36–38]

An AIEE dye, called cyanobis(biphenyl)ethene is reported by Park and coworkers, when it is dispersed in THF/water, nanoparticles were formed and it gives rise to shifted emission and improved fluorescence.[39] Emission in solution and in its solid state results from different emissive processes because of the large shift. P-distyrylbenzene substituted with cyano group was studied by Oelkrug et al.[40] Fluorescence with ϕ_f=0.92 was observed in nonsubstituted p-distyrylbenzene, however, ϕ_f decreases to 0.05-0.1 in aggregation state of nanoparticles.

The behavior of AIEE for the cyano-substituted 1,2-bis(pyridylphenyl)ethene (Figure 7) was revealed because of substitution with cyano groups that have serious quenching on fluorescence in solution but not in the solid state.[41] Red emission was observed after dicyanoethenyl moiety was chosen as an acceptor. (1-cyanotrans-1,2-bis-(4′-methylbiphenyl)ethylene) has a polar and bulky cyano group that contributes a lot to restrict the intermolecular interactions in the aggregated state.[42] Cyano substitution causes the expansion π-conjugation, leading to a redshift.

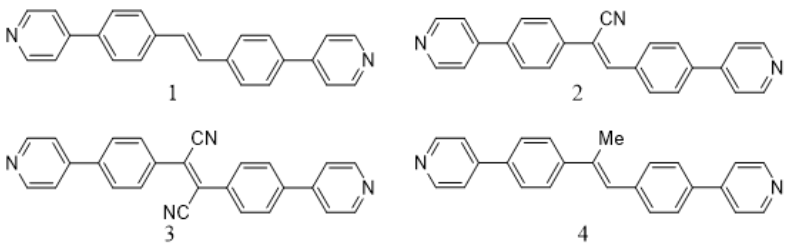

Figure 7 *Cyano-substituted 1,2-bis(pyridylphenyl)ethene.*[41]

2.3. Sulfur-Containing Groups

Sulfur oxides acceptor can regulate the extent of charge transfer of their wave function in its excited state. Anthracene chromophores packed into D-A and D-A-D molecules (Figure 8) have been reported by Pahlavanlu and co-workers.[43]

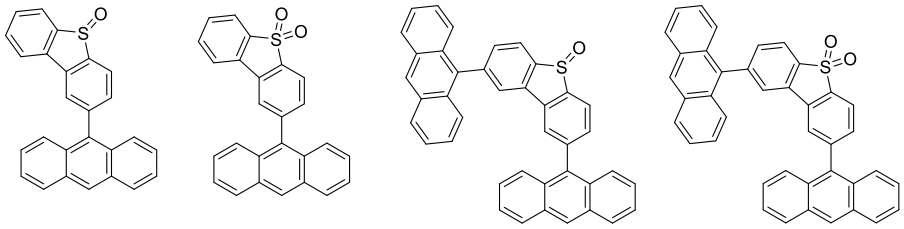

Figure 8 *Anthracene chromophores-based sulfur-containing molecules.*[43]

For other categories, comparing to unoxidized thiophenes, thiophene dioxide has a lower LUMO orbital energy level, so it is an efficient electron acceptor. The extent of charge transfer in D-π-A scheme and electron efficiency of acceptors could be improved by incorporating oxidized sulfur-containing groups. In 2015, Pahlavanlu and coworkers reported a novel method to regulate intramolecular charge transfer character between donor-acceptor among a molecule by controlling the electron deficiency of acceptor.[43] It can be achieved by changing its oxidation state of the acceptor. Anthracene was selected to be an electron donor because its photoluminescence and absorption properties are unique and distinguishable. Dibenzothiophene (DBT) was chosen as an acceptor, in contrast to thiophene, the sulfur atoms in DBT are easily oxidized to open a way to sulfoxide and sulfone derivatives.

Previously, improved photoluminescence among symmetrical sulfur-bridged dimers was reported by Peter R. Christensen and co-workers.[44] Excited-state wave functions were mainly contributed by CT, giving rise to an enhancement in photoluminescence with the increase in the oxidation state of S (S < SO < SO_2). Thiophenes were also reported to undergo oxidation of S,S-dioxides and it shows changes in optoelectronic properties.[45] Photovoltaic applications based on oligothiophene-S,S-dioxides (Figure 9) as electron-acceptor materials were reported by N. Camaioni. Oligothiophene derivatives have stronger electron affinity properties when thienyl rings were transformed into thienyl S, S-dioxide. It dearomatizes the oxidized thiophene ring giving to obvious development of electron affinity and lifted electron dispersion. Narrowed energy gap between p and p* molecular orbitals can be achieved through oligothiophene-S, S-dioxides transformed from oligothiophenes.[46]

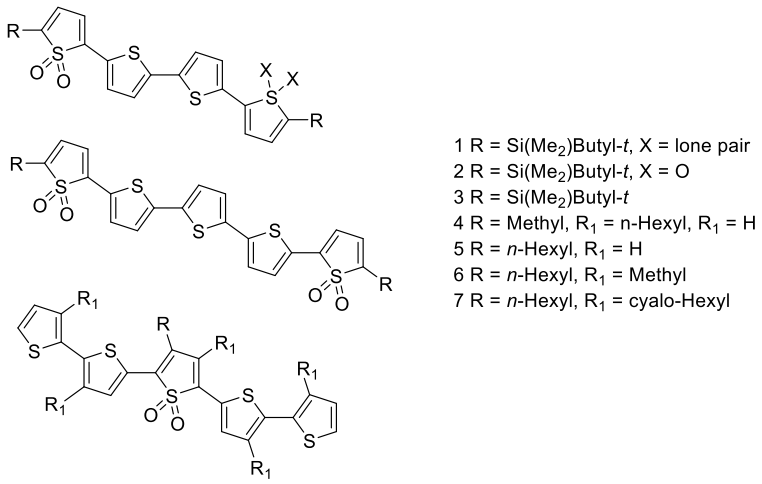

Figure 9 *Molecular structures of the oligothiophene-S, S-dioxides.*

Sulfur-bridged terthiophene dimers have a special feature that can increase the bridging sulfur oxidation state, ranging from sulfide (S) to sulfoxide (SO) and ultimately to sulfone (SO_2). It can modify its electronic coupling of inter-chromophore.

Upon photoexcitation, a delocalized charge resonance state (S_1) can be formed, which relaxes in a short time (<10 ps) to a CT state (S_1*). The degree of charge transfer in S1* can be lifted by increasing the polarity of solvents and the oxidation state of the sulfur group bridge. Controlling of the oxidation state of sulfur bridge gives molecules a way to alter interactions between inter-chromophores in covalent assemblies without changing the molecular polarity or geometry. This tuning provides a new sight for designing functional supermolecules in organic electronics with different functions.

2.3.1 Sulfur-based acceptors in organic photovoltaic (OPV) cells

Organic photovoltaic cells have the potentials to save energy because of their unique properties, such as flexibility, lightweight, plasticity and low environmental impact. The studies of photovoltaic conversion of solar light into electricity are intensively conducted, even though silicon solar cell techniques are well established. Because of the overlap of pπ(C)−dπ(S) orbitals, sulfur atom has π-acceptor characters. Electrons from C=C double bond can be accepted by empty 3d orbitals of divalent sulfur. The construction of the bulk heterojunction solar cell, especially containing sulfur atom, is developed. Those materials rely on the optimization of the spacer by connecting the acceptor unit to the π-conjugated framework to control specific nanophase separation and self-organization. The construction of the first organic heterojunction was conducted by contacting electron acceptor and an electron donor material by Tang in 1986.[48]

Guo et al. reported a single material organic solar cells (SMOSCs) with all-conjugated block copolymers 1 (Figure 10).[49] Through altering acceptor and donor domains, in-plane lamellar morphologies can be achieved by copolymer self-assembly with a

characteristic size of 9 nm (d-spacing of 1 nm). It was proved that the duration of thermal annealing and the temperature shows a significant effect on cell performances increasing power conversion efficiencies (PCE) from 1.5% for 20 min at 100 °C to 2.7% for 10 min at 165 °C.

A category of copolymers with different substituents on the thiophene units and fluorene (2) was also reported by same research group, in order to study their effects of packing of the polymers and solubility.[50] A face-on orientation with π-stacking direction can be realized for all polymers in an out-of-plane direction. These materials in all SMOSCs presented PCE inferior to 0.10%, showing that solubilizing chains have an important impact on phase segregation.

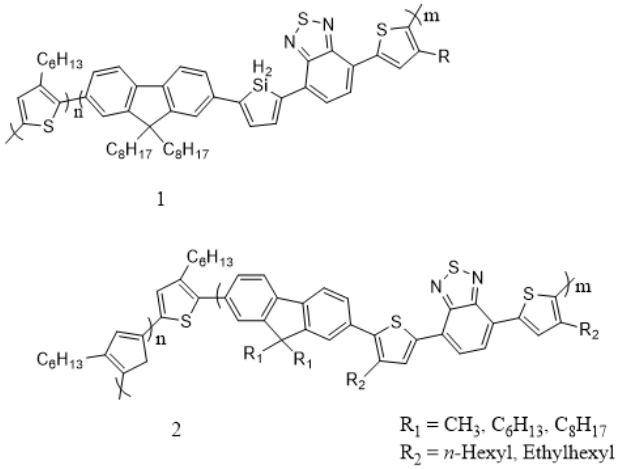

Figure 10 *Chemical structure of copolymers.*[49,50]

2.4. Boron-containing groups

Organoboranes are broadly regarded as boron-containing organometallic schemes because they are regarded as BH_3 derivatives. Organoboranes are usually more susceptible to O_2 because stronger B-O bond is thermodynamically favorable than a common B-C bond. In order to achieve an effective control over the properties of organoboranes, substituents around the boron center should be chosen carefully. For instance, a kinetically stable organoborane was got by connecting mesityl substituents to the boron center. In solid state, interactions between π-π stacking was affected by twisted molecular shape. Commonly, a redshift was detected in its solid state due to the narrower bandgap caused by π-π interactions. Furthermore, a certain π-π interaction, such as H-aggregation, may cause a quench on luminescence in their condensed states of fluorescent materials.[52] Enhanced strong emission quantum yields and higher color purity are observed for organoboranes in the solid state.

In addition, when a boron atom was attached to bulky aromatic units, they prevent the interaction with large Lewis bases or nucleophiles. While the boron center can be

approached by small fluoride and cyanide anions to form stable adducts through a reversible process. Modified optical properties may be caused by the disruption of π-conjugation through boron atom. Small anions can be incorporated into organoboranes to form selective chromogenic and fluorescent sensors.

Borylaniline is the simplest borane-based donor-acceptor organ compound that connects to conjugated systems like aryl group, by a primary-amine and a boryl.[53] Thilagar et al. disclosed that borylanilines (Figure 11, compound 1 and 2)[54] show an important charge separation in its ground state, and it is enhanced further for its excited states.

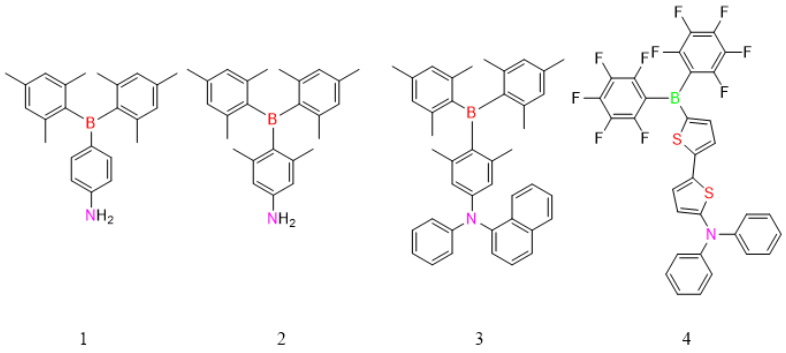

Figure 11 *The compounds of 1, 2, 3 and 4.*[54]

In 2005, a simple donor-acceptor organoborane (compound 3) was chosen by Wang et al., it is applied in a single-layer electroluminescent device.[55] After that, extensive explorations of organoboranes for OLEDs are conducted. Wang et al. also researched the use of metal-containing phosphorescent molecules attached to D-A scheme. To enhance the Lewis acidity of the boryl motif, one efficient way is to use electron-withdrawing groups or atoms around the terminal aryls. In 2007, Jäkle et al. reported the preparation and detailed studies of a D-A system (compound 4) with a terminal -$B(C_6F_5)_2$ unit.[56] This modification leads to a lower HOMO-LUMO gap with a strong bathochromic shift of the absorption and fluorescence bands compared to its non-fluorinated relatives. However, the lower stability was generated by raising electron deficiency of the boron atom compared to non-fluorinated similar compounds.

In the same year, Yamaguchi et al. reported a borylsubstituted molecules which show chromatically pure and strong solid-state emission because solid-state interactions can be prevented by a sterically bulky boryl group. Compounds 1-6[57] on Figure 12 show a fine-tuning of donors at the terminal positions which lead to a wide variety of emission colors, covering the whole visible region of the electromagnetic spectrum (Figure 12).

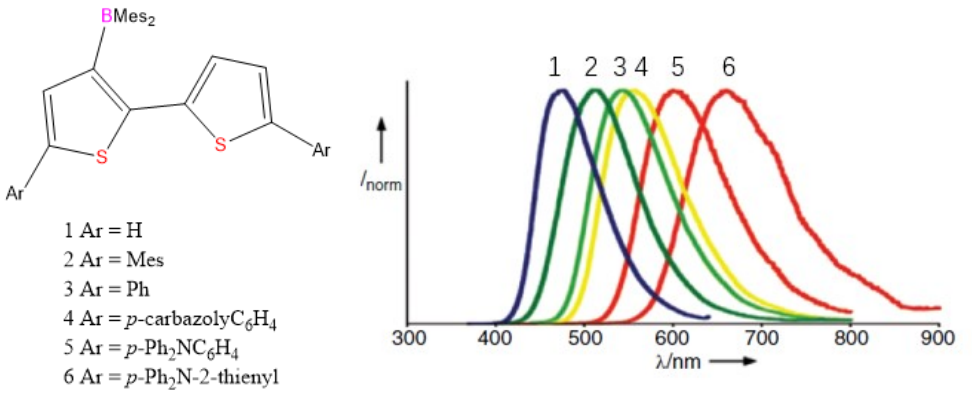

Figure 12 *Structure and fluorescence spectra of 3-borylbithiophene derivatives 1–6.*[57]

2.5. Phosphorus-containing groups

Phosphorus offers a special geometry, when incorporated with conjugated ring systems, an orbital coupling of s*-p* is expected, lowering the energy level of the LUMO. Phosphine oxides further enhance electron-withdrawing abilities of the phosphorus moiety resulting in a tunable photophysical and chemical properties.[58] Organophosphorus fluorophores are found suitable for the application due to favorable characteristics. Excellent fluorescence properties, high absorptivity, great photostability and tunability, make it profitable probe in medicine, environmental indicators, biomolecular tags and cellular stains. High sensitivity and high fluorescence quantum yield make organophosphorus-based probe extensively used for fluorescence detection.

Various phosphorus heterocycles like chiral, helical, annulated and substituted phospholes have been synthesized in order to expand the classes of compounds. The explore of phosphole derivatives and substitution patterns has been developed. Phosphination elimination under high temperatures was carried out for most methods. Two acetylene moieties were connected into an alkyl bridge $(-CH2-)_n$ (n=3, 4), leading to lifted yields and high (regio-) selectivity.

Other synthetic routes like cascade reactions,[59] radical reactions[60], or carboboration followed by rearrangements[59] were also used to get other interesting derivatives. Mixing phosphole building blocks with more complicated structures was prepared to form hybrid carbaboranes[61] in order to create excellent properties.

Optical properties were tuned by the lone pair on phosphorus atom through chemical reactions like borane and metal (Ag, Au, Pd) coordination and oxidation with Se, O and S, or quaternization (MeI, MeOTf, Ph-CH_2X). The larger aromatic systems are often incorporated into (hetero-) cyclic systems and phosphole core. A decrease in aromaticity of the phosphole ring results from aromaticity in an annulated (hetero-)aryl, leading to a change of optical properties. Reduced splitting energy of HOMO-LUMO,

shifted emission maxima as well as red-shifted absorption, was caused by the formation of greater planar p-conjugated systems.

3. Application of organophosphorus chromophores

3.1. Sensing

In a low coordination state of organophosphorus compounds, it is regarded as an outstanding tuning element when connected with other units. Because of the electron-accepting abilities of phosphine oxides, it has been applied in various optical materials. An important application in optoelectronic is single molecular sensing. A direct electronic signal response and induced dramatic changes in optical properties of the whole system were caused by the interactions between lone pairs on p in phospholes and P=O unit of phosphole oxides. But when analyte interacts with attached donor, the CT properties of the phosphole systems can be changed.

Strong fluorescence of benzophosphole derivatives that have strong fluorescence and electron-accepting nature, was studied, especially for benzophosphole oxides.[62–64] 2,3-diarylbenzophosphole oxide was constructed recently by Yamaguchi and co-workers as solvatochromic fluorescent dye with diphenylamino group at 2-position as an electron-donating group (Figure 13).[60]. Their functions as an environment-sensitive biological probe were also studied, they were tested at a variety of solvents with different polarity and they showed large Stokes shifts depending on the solvent polarity, which can be reflected by emission color. The benzophosphole probe have special features, constant absorption around 405 nm and good photostability. Position 3 of 2,3-diarylbenzophosphole oxides was still be studied by the same research group.[65] Matano and co-workers studied the effects on Solvatochromic properties of 2-arylnaphtho[2,3-b]phosphole oxides and 2-arylbenzophosphole, they also use the electron-donating diphenylamino group.[66]

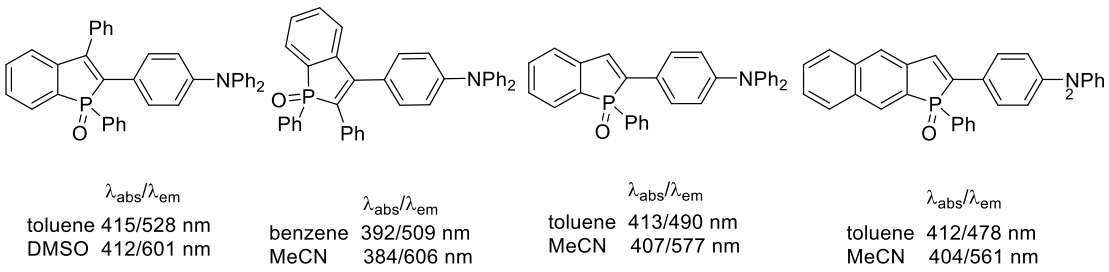

Figure 13 *Solvatochromic fluorescence of benzophosphole oxides .*[67–69]

Purely organic fluorescent systems are widely reported. Analyte detection can be realized by a “turn-on” fluorescence response. Young Hoon Lee reported a novel

method of fluorescence sensor with time-dependent turn-on abilities[70] shown in Figure 14. A donor (carbazole)-acceptor (triarylborane) was added into a phosphine reagent **1** for the application of detecting hydrogen peroxide (H_2O_2). They also demonstrated that the phosphine oxides **2** by H_2O_2 through oxidation of phosphines, giving a turn-on fluorescence within microsecond lifetimes.

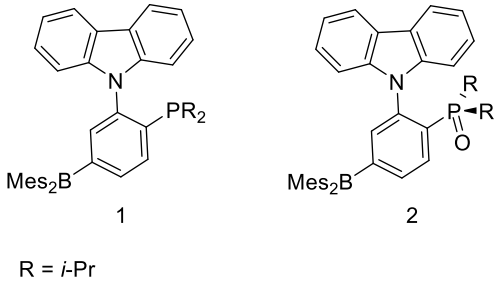

Figure 14 *donor (carbazole)−acceptor (triarylborane) phosphine and phosphine oxides.*

3.2. Optoelectronics

For optoelectronic materials, a good tuning element is organophosphorus, which can be used as molecular building blocks. This tunable and controllable materials are highly desired in an organic light-emitting diodes (OLED) device.

In order to generate white color, phosphole-based materials were searched. Dual emission at 543 and 560 nm from a multilayer OLED was observed by preparing a hybrid thiophene-phosphole-fluorene scheme. white-light emission was observed from the devices. Electron-host and transporting materials in OLEDs were prepared by constructing aromatic molecules functionalized with phosphine oxide.[71]

P-conjugated phosphorus systems are typical benzo- and thieno-fused phosphole derivatives and they have significant potential for organic semiconductors in building blocks. Phosphole-based gold complexes and oligomers show luminescence, reported by Réau and coworkers in 2003. 15a is an organophosphorus emitter example in OLEDs.[72] Baumgartner and coworkers demonstrated a novel category of p-conjugated organophosphorus materials with highly color-tunable capabilities, luminescent dithienophosphole derivatives (Figure 15, b). oxidation to phosphine oxides can tune the electronic properties[73]

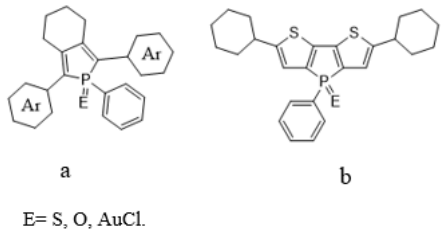

Figure 15 *Examples of phosphole-based luminescent π-conjugated molecules.*[72]

Lee has prepared and reported a novel class of dibenzo-fused phenoxaphosphine and phenothiaphosphine derivatives (Figure 16) used in thermally activated delayed fluorescence emitters[74]. They also tested TADF properties of phosphacyclic emitters by steady-state photophysical and time-resolved measurements, as well as quantum chemical calculations. Based on thermally activated delayed fluorescence (TADF), all these phosphacyclic emitters displayed efficient EL emissions and blue PL. Also, it is shown that subtle chemical tuning in the phosphorus center and connecting heteroatomic parts (–S– vs. –O–) lead to an important influence on the OLED performance and TADF properties. Organophosphorus luminophores showed a promising potential in OLEDs.

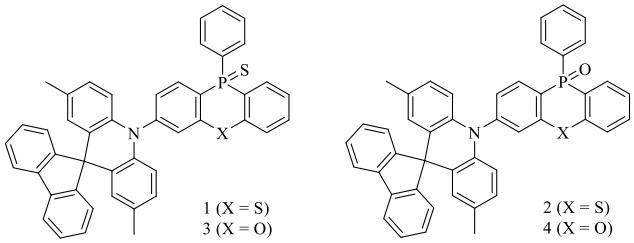

Figure 16 Phosphacycle-related TADF emitters 1–4.

Various phosphine oxides attached to different π-spacers have been investigated. Electron-withdrawing abilities of phosphine oxides promote electron transport. For example, carbazole spacer connects some kind of most efficient phosphine oxide hosts. one of the deep-blue materials is carbazole-based material mCPPO1 (Figure 17, 1)[75] While phosphine oxide material (Figure 17, 2) was shown to be an effective host for blue (dopant FIrpic), red (dopant Ir(piq)3) and green (dopant Ir(ppy)3).[76]

Phosphine oxides combined with carbazoles have often been attached to other scaffolds to generate hosts for phosphorescent complexes. Poriel et al. attached a host consisting of phosphine oxide and carbazole units to a spirobifluorene core (Figure 17, 3).[77] They produced a single-layer green PhOLED (Ir(ppy)3 emitter) with a very high EQE of 13.2%. Xu et al. synthesized a quaternary host system (Figure 17, 4), consisting of a phosphine oxide acceptor, a carbazole donor, a fluorene chromophore, biphenyl π-extender. They can display a blue PhOLED (FIrpic emitter) with an external quantum yield (EQE) of 22.5%.[78] Lee et al. developed a high triplet energy host TSPC (Figure 17, 5) for blue PhOLEDs due to its bulkiness and high triplet energy.[79]

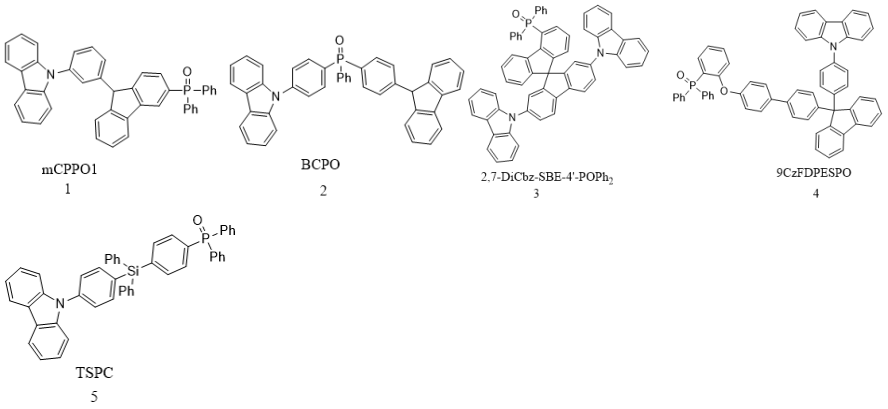

Figure 17 *Selected hosts based on phosphine oxides and carbazole, phosphine oxides and other scaffolds.*[69-79]

3.3. Imaging

Fluorescent dyes needed for biological applications are required to be excited at 650-900 nm at near-infrared range due to low autofluorescence of background and absorption by minimal tissues. Therefore, NIR fluorescent dyes are urgently needed for vivo imaging and diagnosis of diseases.

Rhodamine was widely used in bioimaging, but it still faces an adaunting challenge: the short of absorption and emission wavelengths, normally below 600 nm, are sometimes not suitable in vivo imaging. Xiaoyun reported phosphorus-substituted rhodamines (compound 2, Figure 18)[80] which displays extraordinary long-wavelength fluorescence emission with 140 and 40 nm bathochromic shifts compared to silicon-substituted rhodamine and rhodamine (compound 1), resulting to expanding the region above 700 nm.

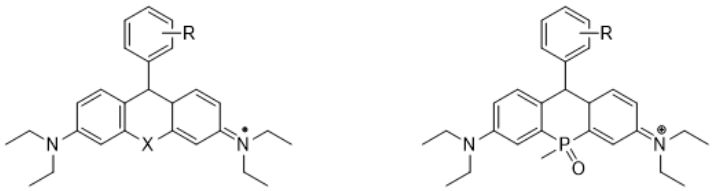

Figure 18 *Rhodamines, silicon-substituted rhodamines and phosphorus-substituted rhodamines.*[81]

Stimulated emission depletion (STED) microscopy for live imaging needs enhanced photostability of a certain fluorescent dye.[81] Chenguang reported excellent small fluorescent molecules that have promising photostability under continuous STED

imaging conditions and in living cells, compared to currently available photostable fluorophores.[82]

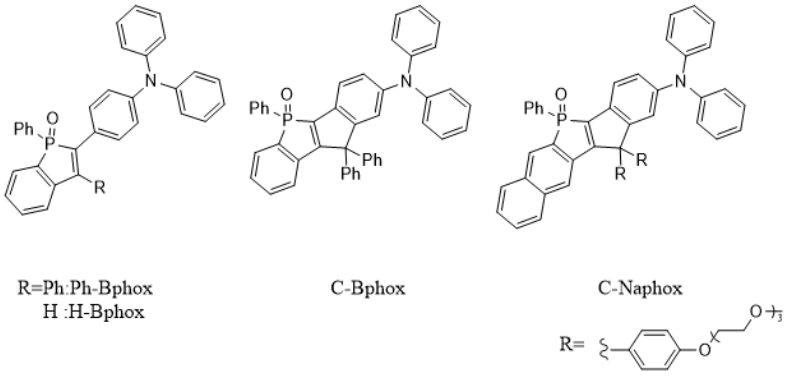

Figure 19 *Phosphole P-oxide fluorescent dyes.*[83]

The combination of the electron-accepting benzophosphole P-oxide with the electron-donating amino moiety (Figure 19) leads to strong fluorescence emissions, having lifted fluorescence quantum yields both in protic and polar solvents.[83] With the increase of solvent polarity, the maximum of emission undergoes an obvious bathochromic shift, changing color from bluish-green to reddish-orange.

4. Conclusion

Even charge transfer has dramatic importance, the studies to these π-stacked molecular or high conjugated system were rare. Bioimaging dyes, photovoltaics and organic electronics need the contribution from π-conjugated donor-acceptor molecules. Such molecules with ICT are also promising candidates in dye-sensitized solar cells and OLEDs. The research into the boron group, cyano group, sulfur-containing group has grown immensely and more practical applications have been applied in modern materials. The continuous researches between synthesis, characterization and applications have enriched the chemistry of fluorescence, with a great number of remarkable results, especially in sensing probe and OLEDs.

The explorations have been conducted from exclusively amine-type donor materials to a wide variety of phosphorus functional groups recently. Then fluorescence of organophosphorus was synthesized and characterized. It is believed that D-A systems containing organoboranes, can realize a range of optoelectronic applications based on the principles of charge storage, separation or changes in photoemission of materials. Recent developments of phosphorus-containing molecules have received a great concern because phosphorus and phosphorus oxides can behave as P-transfer reagents in the synthesis of novel materials to achieve optical properties.

In the future, further tuning of the D-A of organophosphorus is expected to bring further new practical ideas and the combination of conjugated systems with unique π-acceptor

PO will be widely used in phosphorus-based optoelectronics as well as organophosphorus-based sensing.

5. Aims of the work

The develop push-pull (D–π–A) chromophores were studied widely into nitro and cyano groups, elements sulfur and boron, but the investment into phosphorus centers is not sufficient, especially when chalcone is chosen as π spacer. Chalcone provides an excellent conjugation system and its photophysical properties had been studied for many years, which could be used to compare the difference of that when phosphine oxides and phosphoniums were connected to be acceptors. The insufficient studies on phosphine oxides and phosphonium salts as acceptors push me to explore the changes of photophysical properties.

6. Results and Discussion

To develop push-pull (D–π–A) chromophores, we focus our attention on the construction of the phosphonium salts and phosphine oxides decorated by diethylamine groups and linked via a conjugated spacer. When phosphorus was incorporated into the structure, high inversion barrier (30–35 kcal mol^{-1})[84] and tetrahedral shape makes the phosphorus lone pair electrons involved slightly. Moreover, the lone pair electrons on phosphorus have a tendency to quench the luminescence as a result of photoinduced electron transfer and only seldom of these σ^3-λ^3 phosphine materials exhibit high fluorescence quantum yields.[85,86] Oxidation of the phosphines leads to the formation of P=O bond in phosphine oxides, which is very polar and electron-withdrawing because of the high electronegativity of the oxygen atom, causing a lower delocalization within conjugated system. If this electron-withdrawing $Ph_2P(O)$- unit (acceptor) is connected with an organic spacer, it can make the connected spacer electron-deficient and thus improve its electron-transport properties. Moreover, the addition of donors modulates intramolecular charge transfer. In addition, the phosphonium cations, are relatively stronger acceptors due to a positive charge on itself, which could contribute to redshifts of absorption and emission.[87] Although it has obvious properties on electron deficiency of a quaternized $–R_3P^+$ motif, combining with an extended conjugated spacer to generate donor/acceptor chromophores has been seldom reported. These characteristics together are reasons why phosphonium salts/phosphine oxides are suitable candidates for D-A luminophore constructions.[88–92]

With these properties in mind, extensive surveys on the structure with different phosphorus centers (Ph_3P^+-/$Ph_2P(O)$-), donors, as well as a variety of conjugated systems were carried out in order to compare each other in various aspects (Schemes 1,3,4). Initially, the -NEt_2 group as an electron donor was chosen.

6.1. Synthesis of Phosphonium Salts.

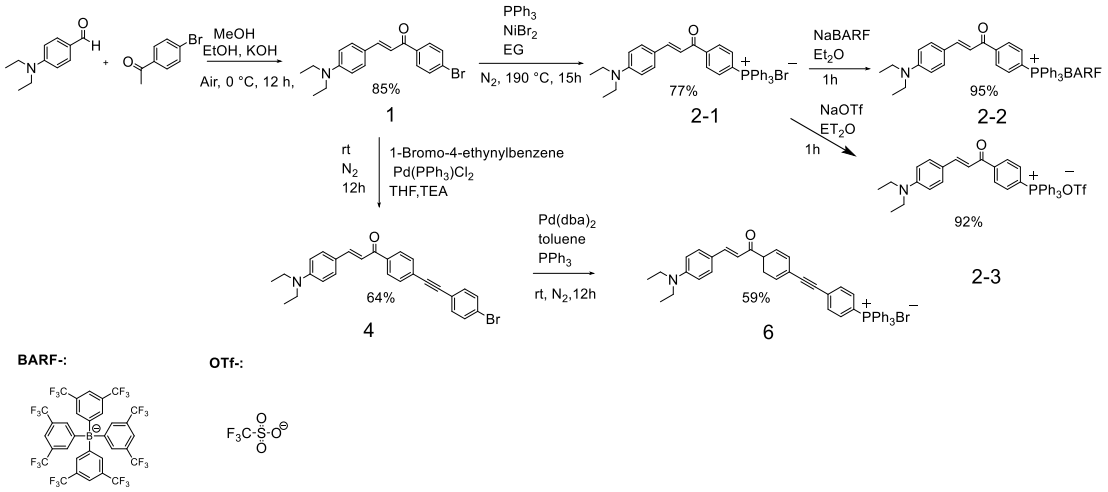

Scheme 1 *Synthetic procedure for phosphonium salts **1**, **2-1**, **2-2**, **2-3**, **4** and **6**.*

Benzylideneacetophenone (i.e. chalcone) conjugated system (Scheme 1), with a double bond connecting to a carbonyl group in the middle of two phenyl groups, was chosen as a basic conjugated spacer. Chalcone is one of the most used π-conjugated structures, being used in various areas, including dye-sensitive solar cells and electronics, and their photophysical properties were also widely studied. A condensation reaction of 4-(diethylamino)benzaldehyde and 4'-bromoacetophenone in the mixture of methanol and ethanol at 0 °C delivers molecule **1** in an appropriate yield of 85%.

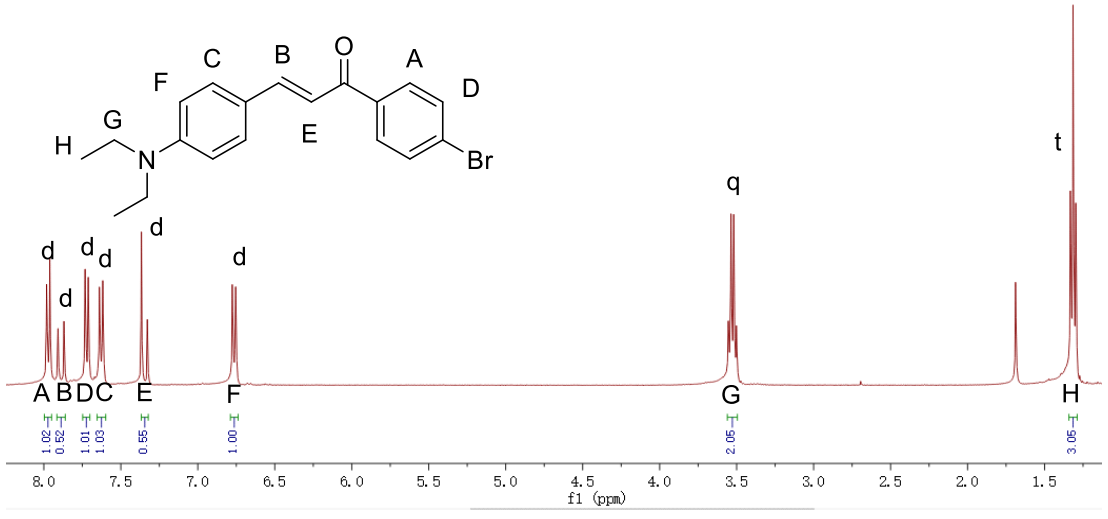

Figure 20 *400 MHz ^{1}H NMR spectrum of **1**, $CDCl_3$, 298 K.*

^{1}H NMR spectrum of the molecule **1**[93] depicted in Figure 20 confirms it's the molecular structure. The hydrogens on the ethyl group are located at positions H and G, and coupled with each other, giving a triplet and a quartet, which can be found in the spectrum. And the integration also proved this. Due to the lone pair on the nitrogen

atom, hydrogens on position F were shielded by electron densities from nearby nitrogen, leading to a shift to upfield, which corresponds to a doublet at 6.76 ppm (J =8.8 Hz, 2H). Its coupled protons locate at C, 7.63 ppm (d, J = 8.8 Hz, 2H). Equivalent hydrogens on position A experiences a de-shielding because of the electron deficiency of the carbonyl group, giving a doublet at 7.97 ppm (J = 8.4 Hz, 2H). Its coupled protons locate at D, 7.72 ppm (d, J = 8.4 Hz, 2H). The integration of a doublet at 7.89 ppm (d, J = 15.2 Hz) shows that there is only one hydrogen as well as the other doublet at 7.35 ppm (d, J = 15.2 Hz). They are hydrogens on position B and E. Those relative peak positions can be found on compounds with similar structures. But sometimes those peaks overlap with peaks from triphenyl group, and cannot be distinguished.

For the construction of compound **2-1**, phosphonium center was introduced into the position of Br- via Ni-catalyzed reaction.[94] Catalyst $NiBr_2$ and solvent ethylene glycol were chosen for classical Horner reaction. Control experiments on different reaction temperatures (150℃, 170℃, 180℃, 190℃, 195℃) were tested to figure out the best reaction temperature. At 150℃, the reaction just starts to proceed, with the color changing of the reaction solution. When rising the temperature from 170℃ to 180℃, the yield, rising from 35% to 70%, was calculated and compared with each other after column chromatography. When rising the temperature from 180℃ to 190℃, the yield rising to 77%, but the content of impurities rises at the same time. At 195℃, the yield decreases to 50%. Finally, the optimized temperature was established at 190℃. A possible mechanism was proposed in Scheme 2.

Under heating to 190℃, ethylene glycol was used to disperse $NiBr_2$, $\{Ni[(CH_2OH)_2]_3\}Br_2$ complex was formed by replacing Br ions with ethylene glycol molecules. While solvent molecules will be replaced because of the higher ligand field of triphenylphosphine. Finally, tetracoordinated $\{Ni(CH_2OH)_2(PPh_3)_2\}Br_2$[95] was formed. $\{Ni(CH_2OH)_2(PPh_3)_2\}^+Br^-$ could be got to start the catalytic cycle. When the oxidation addition of compound **1** happened, a breaking of O-Ni bond occurred. Then compound **2-1** was got and the catalytic cycle continues to be active for the next cycle.

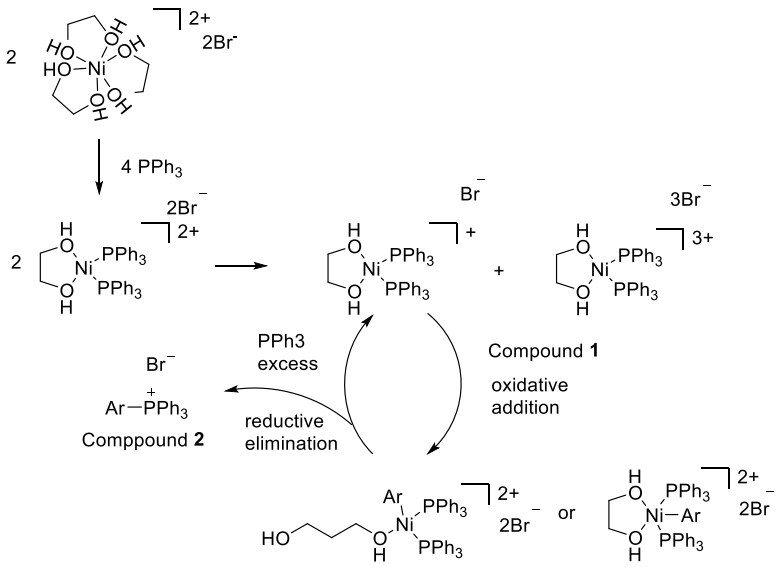

Scheme 2 *Proposed catalytic cycle for the preparation of* ***2-1****.*[96]

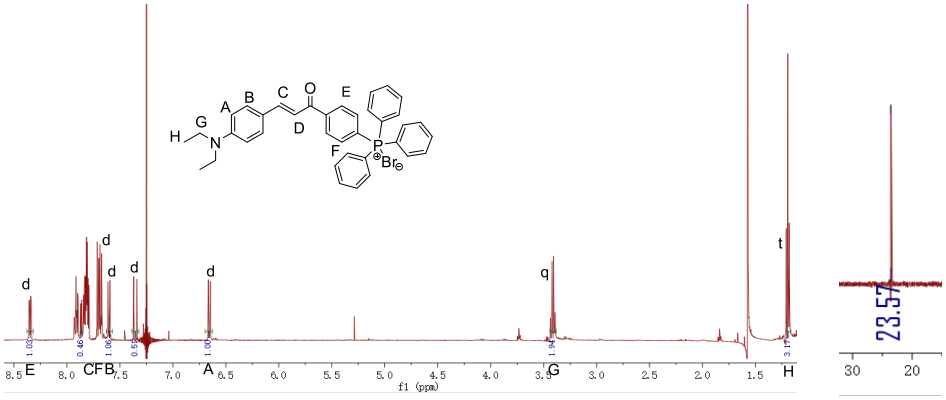

Figure 21 *400 MHz* ^{1}*H (left), 162 MHz* ^{31}*P (right) NMR spectrum of* ***2-1*** *in* $CDCl_3$ *at 298 K.*

^{1}H NMR spectra of the molecule **2-1** were depicted in Figure 21. Due to the lone pair on the nitrogen atom, hydrogens on position A were shielded by electron densities from nearby nitrogen, leading to a shift to upfield, which corresponds to a doublet at 6.65 ppm (J = 7.2 Hz). Doublet (J = 7.2 Hz) at 7.60 ppm is from position B. Equivalent hydrogens on position E experience a de-shielding due to the electron deficiency of carbonyl group, giving a doublet at 8.34 (J = 2.8 Hz, 2H). Its coupled hydrogens locate at F, 7.79 ppm (J = 2.8 Hz, 2H). From the integration, peak at 7.35 ppm corresponds to only one hydrogen at position C (J = 12.4 Hz, 1H). Another doublet from position C may overlap with peaks from three phosphorus-bound phenyl groups. Hydrogens on ethyl group correspond to a triplet and quartet, which are easy to identify. ^{31}P NMR was also tested, which is in accordance with reported data.[97] Elemental analysis was also carried out. Comparing calculated data ($C_{37}H_{35}BrNOP$: C, 71.71; H, 5.70; N, 2.26) and experimental data (C, 70.41; H, 5.81; N, 2.21), the deviation is small, and these two sets of data can confirm the structure of **2-1**.

Ion exchange was further conducted to get compound **2-2**, yield 92 %, and **2-3**, yield, 95%, in order to explore the differences in luminescence caused by different

counterions which could have different interactions in solid state. Mass of negative ions was measured in order to identify the existence of OTf- and BARF-, as well as positive ions to identify the cation compositions. For negative OTf ions, calculated mass is 149.070 a.u., in accords with the measured data, 148.9541 a.u.. For positive ion $[M]^+$, calculated mass is 540.25 a.u. and it is almost the same to measured mass 540.2503 a.u.. Calculated elemental composition for $C_{38}H_{35}F_3NO_4PS$: C, 66.16%; H, 5.13%; N, 2.03%; S, 4.65%. it is close to found data: C, 66.11%; H, 5.34%; N, 2.07%; S, 4.36.

For BARF ion, elemental analysis was conducted to prove the elemental composition of C, H, N. Calculated elemental composition for $C_{69}H_{47}NOPBF_{24}$ is C, 59.03%; H, 3.37%; N, 1.00%, which is close to found data: C, 59.92%; H, 3.40%; N, 0.98%. For negative BARF- ion, the measured mass is 863.0883 a.u. (calcd 863.211 a.u.). For positive ion $[M]^+$, calculated mass is the same as measured data, 540.2503 a.u..

Compared to compound **1**, a more extended conjugated system **4**, yield (64%), was constructed for the synthesis of final desired phosphonium salt **6**. Under the catalysis of $Pd(PPh_3)Cl_2$, a coupling reaction occurs between compound **1** and 1-Bromo-4-ethynylbenzene. Then the transformation of compound **4** to **6** requires a zero-valent palladium, like $Pd_2(dba)_3$, $Pd(dba)_2$.[94] In my case $Pd(dba)_2$ was chosen. It was also carried out under nitrogen to avoid the oxidation of Pd^0 to Pd^{2+} which form an inactive catalyst for phosphonium transformation. The **4** reacted with triphenylphosphine under the presence of $Pd(dba)_2$ in toluene at 130 °C for 15 h, yield 59%.

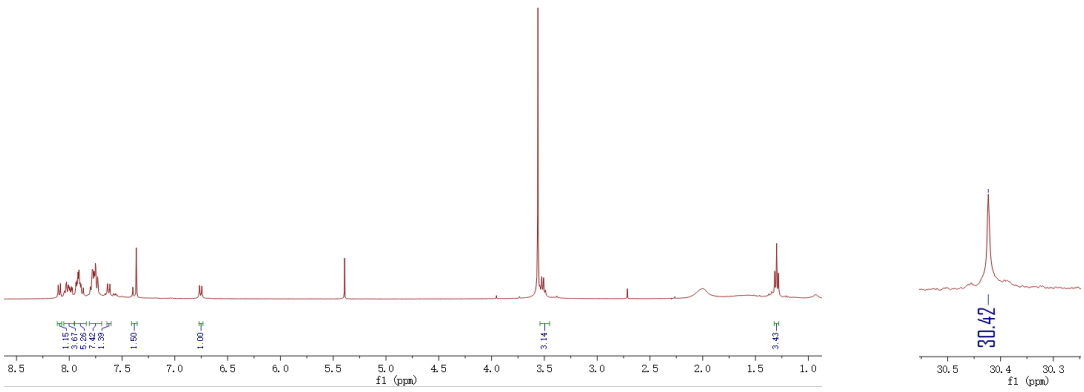

Figure 22 *400 MHz ^1H (left) and 162 MHz ^{31}P (right) NMR spectrum of* ***6*** *in $CDCl_3$ at 298 K.*

The ^1H NMR spectra of compound **6** (Figure 22) is not easily distinguishable due to the existence of more phenyl groups. They have a similar chemical shift, leading to three main overlap areas. In order to confirm the identity, other effective analysis methods were chosen, they are mass and elemental analysis. For positive cations, a measured mass is 719.20 a.u., its original mass is also 719.20 a.u.. Its elemental composition was also calculated, C, 75.08%; H, 5.47%; Br, 10.97%; N, 1.94%; O, 2.22%, which is almost same as found data, C, 75.00; H, 5.45; Br, 11.09; N, 1.94; O, 2.22; P, 4.30. ^{31}P NMR was also tested, there is only one peak at 22.62 ppm (no internal standard was

used for chemical shift, it needs to subtract 7.8 ppm form 30.42 ppm) and it is close to reported data.[97]

6.2. Synthesis of Phosphine Oxides

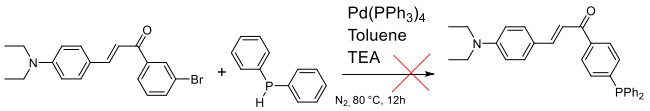

Scheme 3 *Failed trial for the synthesis of phosphine that can be oxidized into compound **3**.*

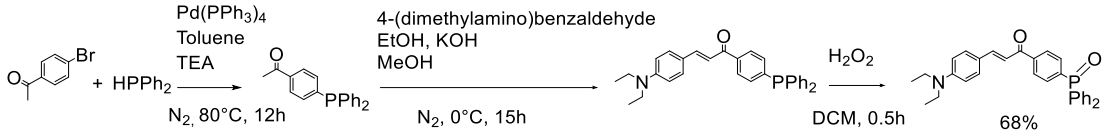

Scheme 4 *Synthetic procedure for phosphine oxide 3.*

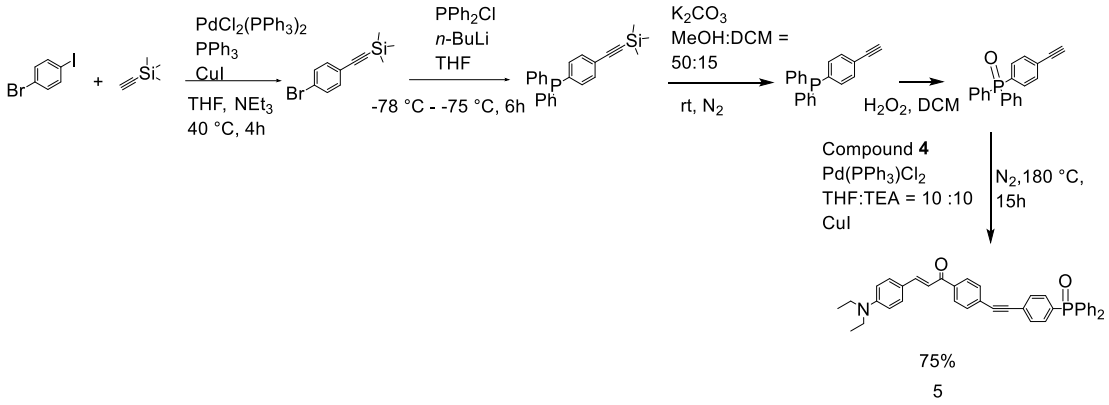

Scheme 5 *Synthetic procedure for phosphine oxide **5**.*

Compound **3** has the same conjugated system compared to compound **2-1** apart from the phosphorus center. Different assumptions (Scheme 3 and 4) were tested: the first one is that diphenylphosphine reacts directly with compound **2-1**. Unfortunately, it only gives minor product, yield, 0.0966%. Then the other possible synthesis pathway was proposed on Scheme 4. 4-bromoacetophenone reacts with diphenylphosphine to get 1-[4-(Diphenylphosphino)phenyl]ethenone.[98] The reaction conditions were strictly controlled under an inert environment to avoid the oxidation of diphenylphosphino group. Then 1-[4-(Diphenylphosphinyl)phenyl]ethenone reacts with 4-(diethylamino)benzaldehyde. Finally, oxidizing the diphenylphosphino group with H_2O_2 followed by a fast column chromatography to obtain **3**.

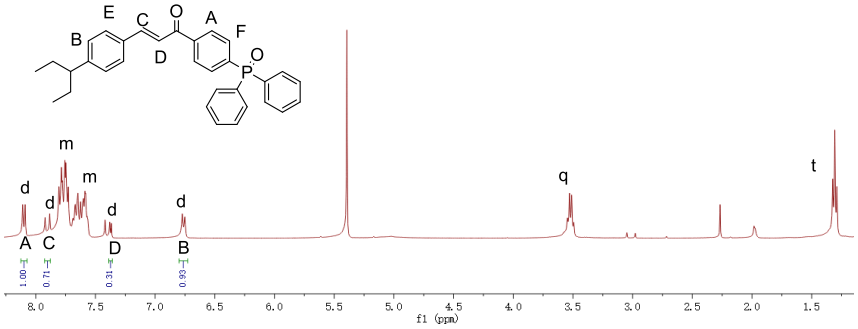

Figure 23 *400 MHz ^1H NMR spectrum of **3**, $CDCl_3$, 298 K.*

Compound **3** has two phosphorus-bound phenyl groups, which causes the overlap of peaks, giving multiple peaks. ^{1}H NMR spectrum of **3** was depicted in Figure 23, A doublet at δ = 8.10 (J = 8.0 Hz) belongs to hydrogen at position A because of the de-shielding of a neighboring electron-deficient carbonyl group. Another doublet at 6.76 ppm (J = 8.8 Hz) is from hydrogen at position B, caused by a neighboring electron-rich nitrogen atom. Lone pair electrons cause shielding of an external field, moving to upfield. Integration shows that doublet at 7.90 (J = 15.6 Hz) and 7.37 (J = 15.6 Hz) corresponding to the hydrogen at position C and D, because of the identical coupling constant.

Compounds **5** and **6** also have similar conjugated system apart, but decorated with Ph_2PO- and PPh_3- groups, respectively. The procedures for the construction of **5** were shown on Scheme 5. The main effort is done to get 4-(Ethynylphenyl)diphenylphosphine oxide. The synthesis of 4-(trimethylsilylethynyl)bromo benzene was the first step as well as a vital step. On the catalysis of $PdCl_2(PPh_3)_2$ and CuI, 4-iodo-bromobenzene reacted with trimethylsilylacetylene at the temperature of the ice bath. Due to the different activities of bromide and iodine atom, strict control of the molar ratio (1.5/1) of 4-iodo-bromobenzene and trimethylsilylacetylene was fundamental for the successful synthesis of 4-(trimethylsilylethynyl)bromo benzene.[99] If the former was far more excess, the relatively more active iodine atom can react with trimethylsilylacetylene. If the molar ration was not strictly controlled, the trimethylsilylacetylene will react further with the inert bromide atom, leading to another product, 1,4-bis[(trimethylsilyl)ethynyl]benzene. It will give a mixture. So strict control of ratio is the one of most fundamental requirements.

Lithiation of phenyl carbon and substitution of the Br^- with Li^+ happens in the second step. Electrophilic substitution occurred when the electron-poor phosphorus center of chlorodiphenylphosphine attacks the electron-rich carbanion, giving 4-(Ethynylphenyl)diphenylphosphine. 4-(Ethynylphenyl)diphenylphosphine was prepared according to the published literature.[100] Then, adding K_2CO_3 to methanolic solution removes the trimethylsilyl group. Oxidation of trivalent phosphorus center by means of H_2O_2 allows to get 4-(Ethynylphenyl)diphenylphosphine oxide[101]. The final

step is to combine the two molecules via Sonogashira coupling method under the catalysis of $Pd(PPh_3)Cl_2$ and CuI at room temperature, yield 75%.

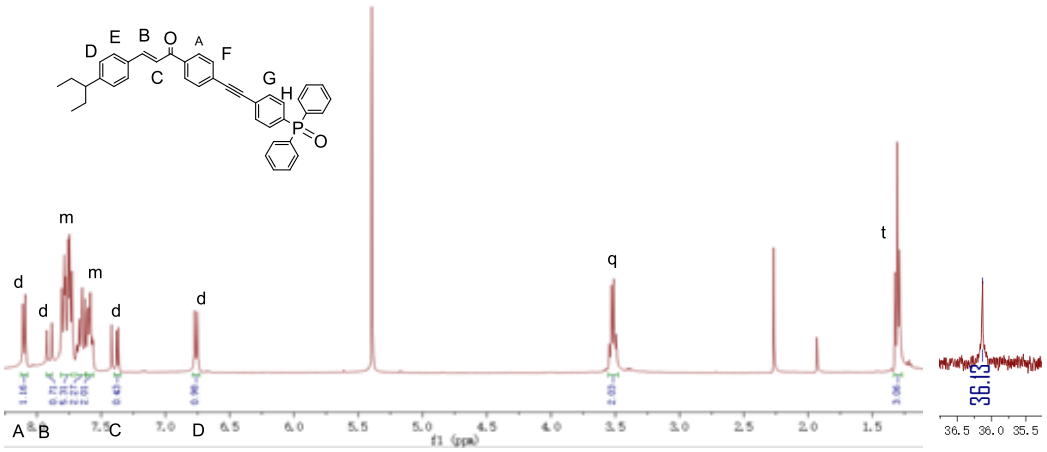

Figure 24 *400 MHz ^1H (left), 162 MHz {^{31}P right} NMR spectrum of* ***5****, $CDCl_3$, 298 K.*

Compound **5** has a longer conjugation system than compound **3**, which still causes the overlap of peaks (Figure 24). A doublet at δ = 8.10 (J = 8.4 Hz) belongs to hydrogen at position A because of the de-shielding of a neighboring electron-deficient carbonyl group. Another doublet at 6.76 ppm is from hydrogen at position D, caused by a neighboring electron-rich nitrogen atom. Lone pair electrons cause shielding of external field, moving to upfield. Chemical shift on the phenyl group is similar due to the equivalent chemical environment. Doublets at 7.90 ppm and 7.40 ppm have same coupling constant J = 15.6 Hz corresponding to position B and C. Apart from the hydrogen on position A and D that have distinct chemical environment because of their neighboring electron density factor, and position B and C have large coupling constant, other hydrogens from phenyl groups give large overlaps. ^{31}P NMR was also tested, single peak at 28.33 ppm.[102]

6.3. Unsuccessful Results

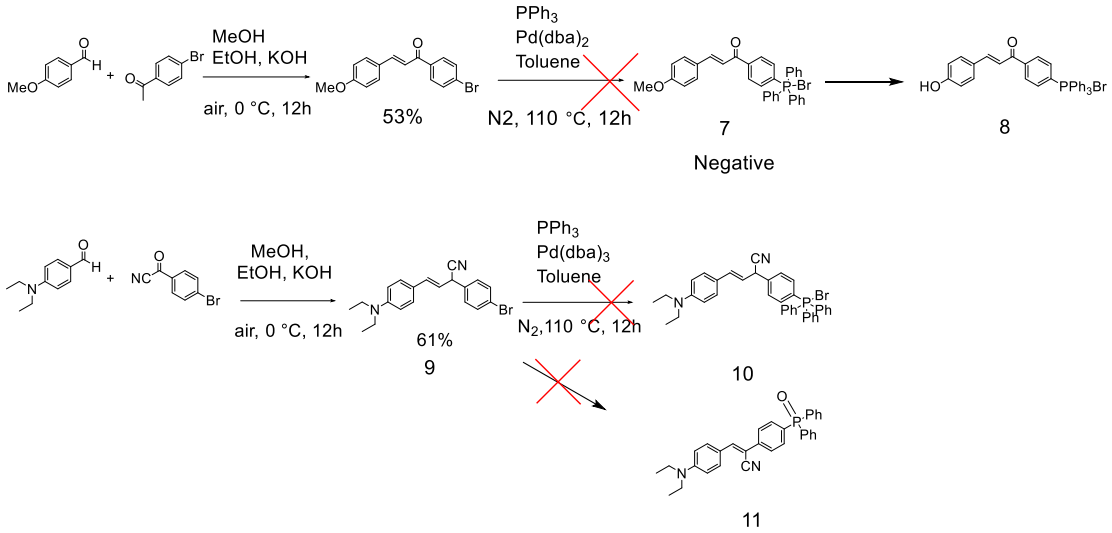

Scheme 6 *Failed attempts to prepare compounds* ***7-11***.

Compounds **1-6** show positive results after various attempts. Even though reactions should happen from theoretical points of views in some cases, syntheses of compounds **7-11** were failed after a series of attempts (Scheme 6), I cannot manage to get separable and pure desired products.

Compounds **8** and **2-1** have same conjugated systems and electron acceptors, but distinct electron donors. The electron donor for compound **2-1** is NEt_2 group, but a hydroxyl group for compound **8**. Diethylamino group and hydroxyl group are all strong electron-donating groups. Although the two structures are similar, the reaction conditions are not applicable to the other. The desired product **8** has a hydroxyl group as electron donor. For the first step, the reaction conditions are totally the same, KOH dissolved MeOH and EtOH at the temperature of ice bath, yield, followed by the substitution of the triphenylphosphine group. Unfortunately, only trace amount of compound **7** was got. Then a new method[103] was tried, using phenol as a solvent without the catalyst. It has shown that there is no compound **7** generated. Therefore, a negative result was got. Then the next step cannot be proceeded further, compound **8** cannot be obtained through two trials.

In scheme **5**, the conjugated system was changed by replacing the carbonyl group with cyano group, but the same electron donors and electron acceptors as for compounds **2** and **4**. From the ^{1}H NMR spectra (Figure 25), it shows that the product contains a mixture of *Z, E* isomers, and the minor Z isomer cannot be separated. Further experiments for the synthesis of phosphonium **10** were conducted. From ^{1}H NMR analysis (Figure 26), it showed that there are two sets of signals but different chemical shifts. The mixture cannot be separated and purified by silica gel chromatography. It is also the case for phosphine oxide **11**, they are failed results.

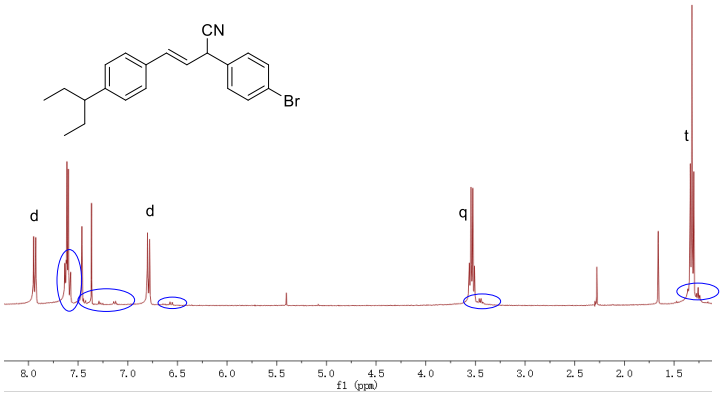

Figure 25 *400 MHz ^{1}H NMR spectrum of* ***9,*** *$CDCl_3$, 298 K.*

Peaks circled have the same multiplicity with nearby main peaks, it may be caused by the introduction of CN- group because the CN- group has a strong electron-withdrawing ability, which can change surrounding electron densities. Those peaks cannot be removed from silica gel chromatography and the situation gets worse for ^{1}H NMR spectrum of **10** (Figure 26). In the process of synthesizing processes, heating to 110℃ was needed, these energies for the cis and trans transformation were provided by heating, giving higher proportion of cis or trans forms.

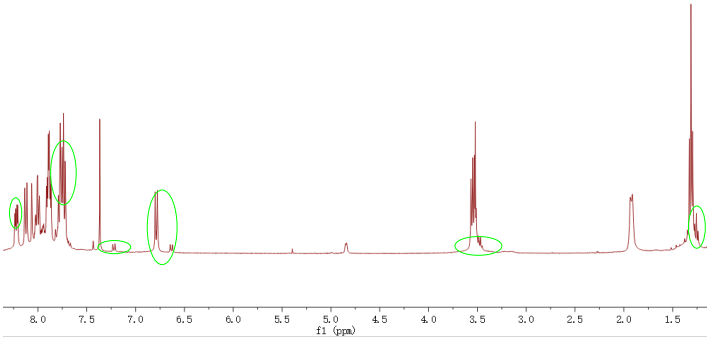

Figure 26 *400 MHz ^{1}H NMR spectrum of* ***10,*** *$CDCl_3$, 298 K.*

7. Single Crystal Analysis

The suitable crystal for single X-Ray analysis was prepared by slow evaporation of the dichloromethane/hexane mixture of **3** at +5℃. It has good solubility on dichloromethane but bad in hexane. Dissolving compound **3** in dichloromethane and then adding hexane (volume ratio: 1/1) carefully to disperse solute molecules. Finally, orange crystals were formed in several days.

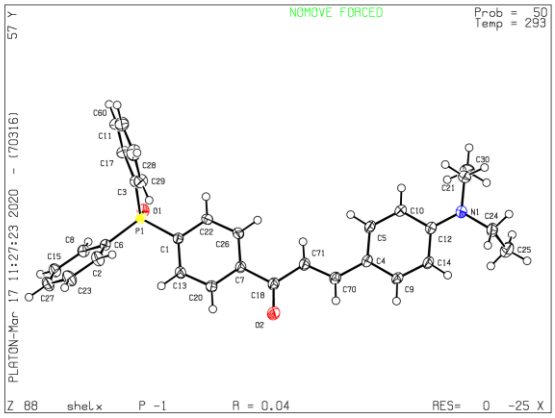

Figure 27 Molecular views of compound **3** (white: hydrogen, red: oxygen, yellow: phosphorus, blue: nitrogen and the rest atoms are carbon)

The XRD structural analysis reveals its crystalline data with high accuracy and these crystallographic data allow for clear distinguishing of atoms, like phosphorus, oxygen and nitrogen atoms. The molecular structure accords to the ^{1}H NMR analysis.

Table 1 *Parameters of the crystal unit cell for compound **3**.*

Length	a=10.3626(11)	b=11.2713(12)	c=11.8475(12)
Angles	α=68.758(3)	β=74.401(3)	γ=83.980(3)

From these data (Table 1), it belongs to the triclinic crystal system due to the total irregular angles and length of the unit cell. Bond length for P-C varies from P_1-C_6, 1.8020 Å to P_1-C_1, 1.8074 Å[104] and other interested bond length is also shown: C_{18}=O_2, 1.230 Å, average C-C bond 1.4082 Å. The angle of $C_1P_1C_3$ is 106.59°, 108.40° for $C_1P_1C_6$.

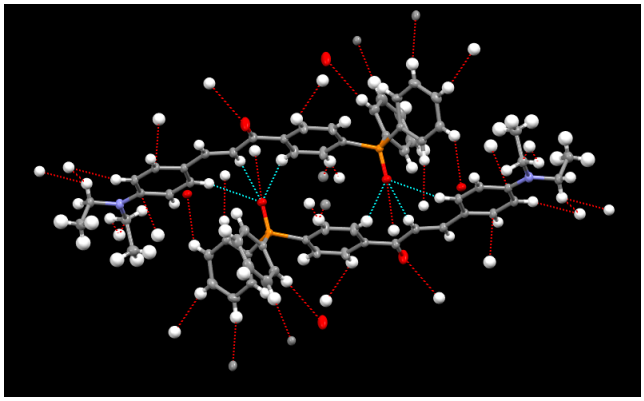

Figure 28 *Dimer packing pattern of crystal molecules.*

There is a dimer packing pattern for crystal molecules shown in Figure 28, it is mainly because of the interaction between two molecules, the spatial position also contributes part of the effort. The interaction of P=O---H and H---O=C draws tensely every two facing molecules to offer the highest extent of packing. In addition, the dislocation between two molecules also provides the best interaction positions, keeping ethyl

groups at the two ends to ensure that the molecules have the closest connection. It also shows a flat conjugated spacer. Any rotations on double and single bonds could lead to a loss of conjugations, which will be energetically unfavorable for the system. Only a flat spacer could provide the lowest energy.

8. Photophysical Properties

The incorporation of organophosphorus centers into a largely π-conjugated system has become a meaningful research area for the construction and tuning of a large variety of chromophores. Those modifications want to lower the energy levels of the LUMO and then to change the photoluminescence properties. The involvement of electron-deficient phosphorus centers (phosphine oxides and phosphonium salts) into the conjugated systems decorated with donor could enhance the charge transfer (CT) characteristics. Upon photoexcitation, electron density movies from electron-rich part (donor) to electron-deficient part (acceptor). They are markedly stronger acceptors compared to the neutral oxide/sulfide species, phosphonium cations can give redshifts on absorption and emission spectra.[105]

Connecting an electron-deficient P center (A) with an electron-rich group (D) through a π-conjugated spacer provides a charge separation in the polarized D-π-A species. The energy levels of HOMO and LUMO are mainly localized on the D and A moieties, respectively. The excitation of such molecules with a suitable wavelength of light can induce an ICT process as well as their unique luminescence properties such as thermochromism, emission, dual emission, multi-photon absorption, solvatochromism (effects of polarity/viscosity of the solvent). The acceptor (A) and the donor (D) are connected by a spacer, but no effective interaction among their ground state, it is proved to be feasible energetically to occur CT in their excited state.[106–108]

Significant charge redistribution appears in the molecule when the electron density is transferred from the electron efficient diethylamine group (-NEt_2) to the electron-deficient phosphonium (-$^{+}PPh_3$) or phosphine oxides (-PPh_2O) upon photoexcitation. The energy of ICT process mainly relays on the strength of donor and acceptor, for example, the relative size of the energy of the HOMO of donor and LUMO of acceptor and the degree of electronic coupling between spacer orbitals. The spacer causes the coupling of the two groups and the conjugated system is alike an insulator or a conductor depending on the coupling magnitude. The coupling between both donor and acceptor groups are relevant to transition energies as well as oscillatory strengths. The weaker coupling in the ground state, the smaller the excitation energy.[109] Therefore, the photophysical properties were studied in these three aspects: donor types, the length of conjugations and acceptor types.

8.1. Absorption Spectra

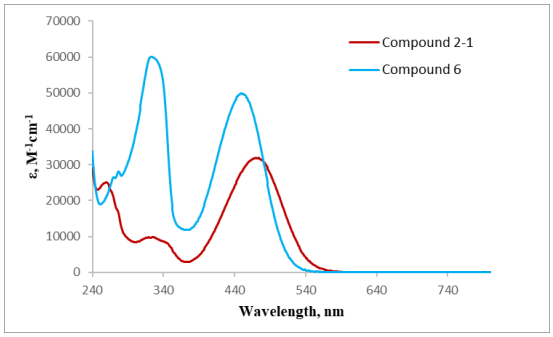

Figure 29a *Absorption spectra of compound* ***2-1*** *and* ***6*** *in chloroform.*

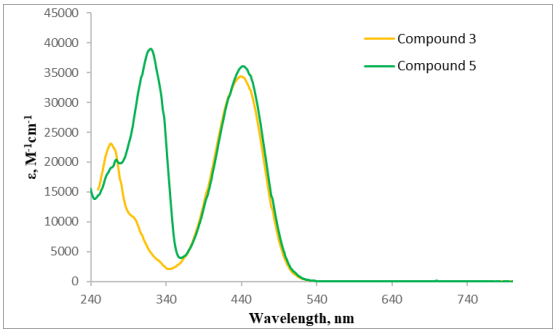

Figure 29b *Absorption spectra of compound* ***3*** *and* ***5*** *in chloroform.*

The absorbance spectrum of compound **2-1**, measured in dichloromethane, is depicted in Figure 29a. There are several peaks found and a low energy peak located at 470 nm, most probably, it is attributed to intramolecular charge transfer transitions. Higher energy peaks, located at 322 nm of **6** and 320 nm of **5** may be π-π*, may belong to π-π* comparable to reported data.[110]

The absorption maxima relay on the nature of the connected substituents and the lengths of the conjugated spacer. Redshift in the absorption band might be expected with increasing spacer length (i.e. **2-1**→**6** and **3**→**5**). While Figure 29a shows an opposite result with the extension of the conjugation, a blue shift was observed, the ICT peak at 470 nm of **2-1** shifted to 450 nm of **6** in chloroform, when the conjugation length becomes longer. Figure 26b shows a tiny absorption wavelength shift from 440 nm of **3** to 443 nm of **5** with the elongation of the conjugation system. Like food dyes, shifting from 560 to 650 nm was observed,[111] their peak wavelengths tend to be shifted toward the long-wavelength regions.

The higher degree of the π-conjugated system, the low-lying π→π* transition gap will be lower and consequently corresponding to the lower energy wavelength. The π→π* transition in less conjugated compound **2-1** is energetically more difficult due to its less conjugated electron distributions and could absorb shorter wavelengths with high energy to reach that energy barrier, which conforms to the absorption band in Figure 29b. There is also an absorption peak around a wavelength 259 nm. But the intensity is not as strong as ICT process that has a more intense absorption at wavelength 470nm, which corresponds to a lower transition energy. The n→π* transition still exists, even though it is not prominent compared to the other two pathways.

Normally, with the rise of conjugation extent, the energy difference between ground states at donors and excited states at acceptors could get smaller.[112] When the conjugated π-system is extended to a larger level in compound **5** and **6**, there is an increase in the degree of the π-electron system. The π→π* transition energy gap could

become narrower, leading to a shift of the absorption spectra to longer wavelengths and the absorption intensity becomes stronger due to the easier electron transition.

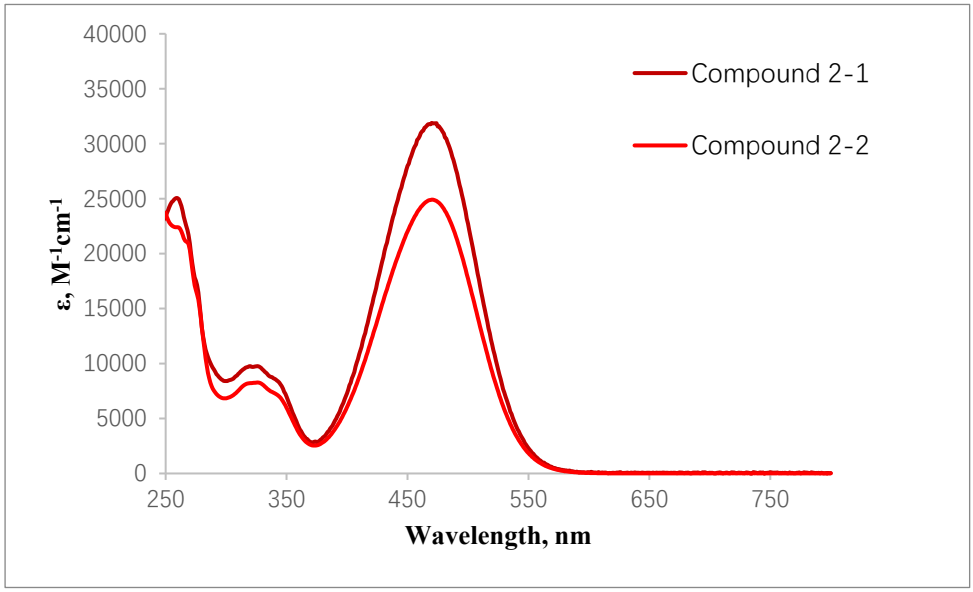

Figure 30 *The absorption spectra of counterion in compound* ***2-1*** *and* ***2-2*** *in chloroform.*

Counterions also cause different intermolecular interactions. The spectral signatures were found to be dependent on the nature of counterions, leading to significant emission color changes. The role of fluorine in counterions is particularly important because fluorinated groups have powerful electron-withdrawing properties, super-hydrophobic abilities and orthogonal to aqueous.[113] Counterion influence was shown in Figure 30, when Br- was replaced with BARF-, the maxima of ICT peak moved from 474 nm at **2-1** to 470 nm at **2-2**. The ground state of **2-2** was more stabilized compared to **2-1** and high energy wavelength light was needed to reach the excitation, therefore a small blue shift is observed. And there is also a decrease in absorption intensity.

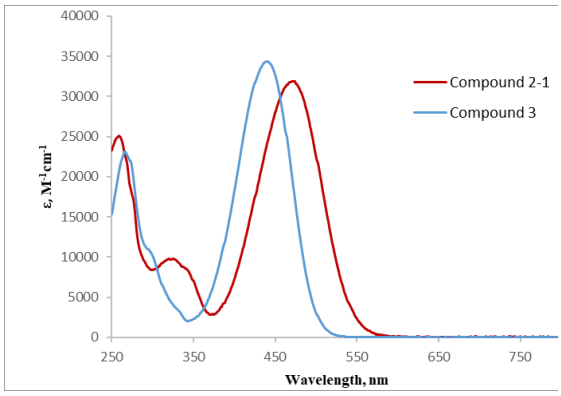

Figure 31a *The absorption spectra of compound* ***2-1*** *and* ***3*** *in chloroform.*

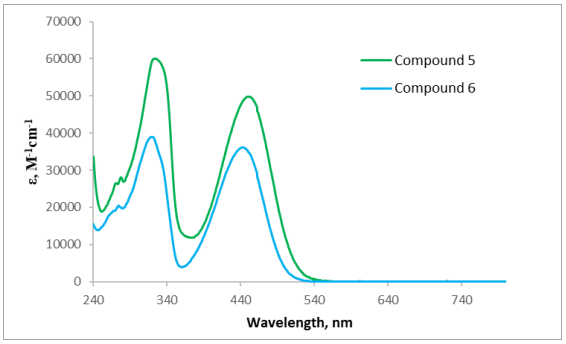

Figure 31b *The absorption spectra of compound* ***5*** *and* ***6*** *in chloroform*

Furthermore, a bathochromic shift is observed with changing electron acceptor from -PPh_2O to -$PPh3^+$ (**3→2-1**, **5→**6). The electron-withdrawing ability of -PPh_3^+ cation center at compound **2-1** is relatively stronger compared to -PPh_2O center at compound **3**. The stronger acceptor -$PPh3^+$ decrease energy of LUMO orbitals, leading to narrower energy between unchanged HOMO and decreased LUMO (Figure 31a). There is a redshift when phosphine oxide was changed to phosphonium salt, from 438 nm to 474 nm, and an intensity decrease is also observed. Similarly, a redshift on **5** and **6** were shown in Figure 31b, from 443 nm to 452 nm, when the conjugation system is enlarged at **5** and **6** compared to **2-1** and **3**, respectively.

8.2. Solvent and pH Effects on ICT Process

The promotion of an electron from its ground state orbitals to its excited state orbitals could be achieved by the excitation of a fluorophore. If the ground state orbitals and excited state orbitals are separated by a spacer, the change of dipole moment for a fluorophore can be finished instantaneously. When an electron-withdrawing group (e.g., >C=O, -CN) and an electron-donating group (e.g., -NH_2, -NEt_2,) were connected through a spacer, the dipole moment becomes larger. Therefore, a disequilibrium state of excited state could be reached because of the interaction of dipole moments with surrounding solvent molecules.

The solvent dependence[114] of various compounds was also tested and observed in different solvents. Broadened absorption/fluorescence bands were observed and this may be caused by fluctuations of solvation shells. In addition, changes in the nature of solvent and composition can induce absorption/emission shifts.[115] When solvent molecules surround a solute, solute-solvent interactions can stabilize their ground and excited states, which mainly relays on their chemical nature. Van der Waals interactions and hydrogen bonding are the most common solute-solvent interactions

The interaction between solute and solvent is tested at different solvents with different polarities. The spectral shift, intensity and shape are influenced by the polarity of solvents and acidity of the medium. Figures 32 and 33 have shown a minor spectral shift and a sharp decline of ICT band, which is found to be sensitive toward solvent polarity.

8.2.1.Effects of polarity

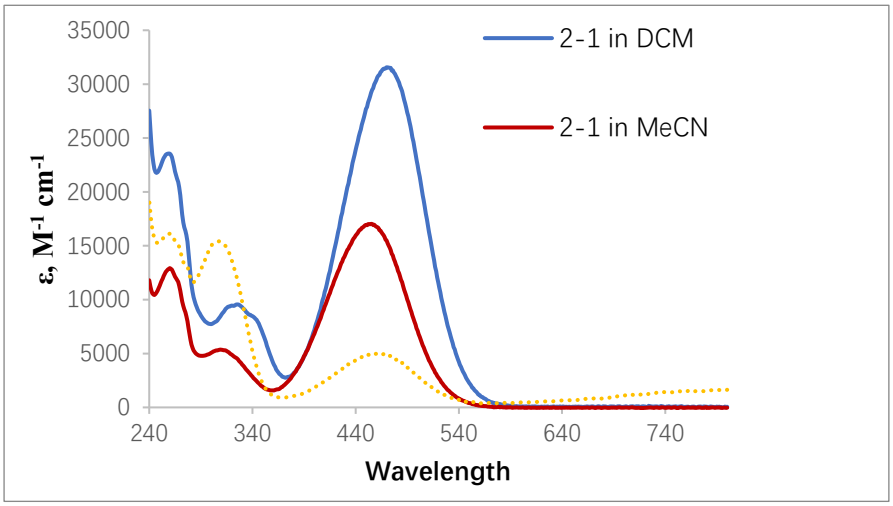

Figure 32 *Absorption band of compound* ***2-1*** *in different polar solutions: DCM, MeCN and the mixture of MeCN and hypophosphorous acid.*

In relative nonpolar DCM solution, the maximum of absorption is at 470 nm and molar absorptivity ε reached 31566 $M^{-1}cm^{-1}$. When solvents change from DCM (relative polarity, 3.4) to MeCN (relative polarity, 6.2), polarity increases correspondingly. The dipole moment of the compound **2-1** is quite large because of the separation of the positively charged center on phosphorus and negative charge on the nitrogen atom. The ground state can be stabilized through the interaction with more polar solvents. Much larger dipole moments have stronger interactions for compound **2-1**, the ground state then is stabilized. The energy level of the ground state is reduced, but the energy level of an excited state remains unchanged. This means that the energy gap becomes larger (Scheme 8), corresponding to a blue shift to shorter wavelength range, resulting in a shift from 470 nm in DCM to 455 nm in MeCN. Negative Solvatochromism was also observed on anionic thiazole-based dyes,[116] with a negative solvatochromism of 114 nm, which varies from 624 nm at tetramethylurea to 510 nm at methanol.

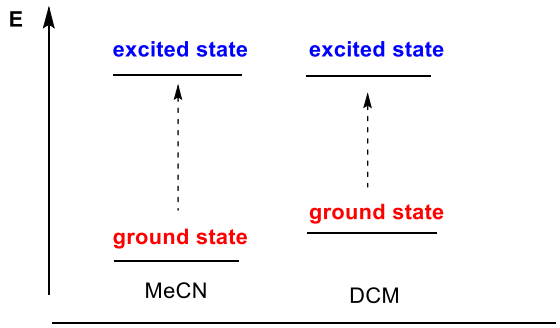

Scheme *7 Energy levels of ground state and excited state of* ***2-1*** *in MeCN and DCM.*

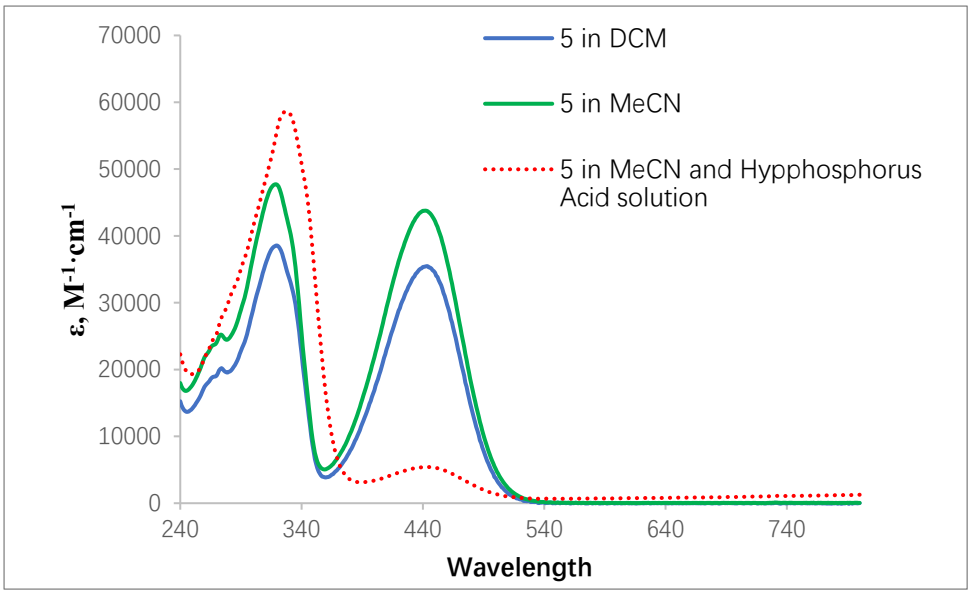

Figure 33 *Absorption band of compound* ***5*** *in different polar solutions: DCM, MeCN and the mixture of MeCN and hypophosphorous acid.*

Table 2 *The maximum absorption wavelength* λ_{max} *(nm) and molar absorptivity ε* ($M^{-1}cm^{-1}$) *of ICT process on compound* ***2-1*** *and* ***5*** *in three different solutions with different polarity.*

Different solutions	λ_{max} and ε of **2-1**	λ_{max} and ε of **5**
Solution 1	470nm, ε=31566	443nm, ε=35465
Solution 2	455nm, ε=17031	442nm, ε=43774
Solution 3	461nm, ε=5028	443nm, ε=5422

In compound **2-1**, the acceptor is a phosphonium cation, thus effects on drawing electrons to itself are stronger compared to compound **5**. The electron-withdrawing ability of acceptor on compound **5** is weaker, which contributes to a weak redshift of ICT from MeCN, 442 nm to DCM, 443 nm (Table 2). The extent of conjugation at compound **5** is higher than that in compound **2-1**, which means that energy levels of excited state π* could be lower. The transition of lone pair electrons to the lower energy of excited state could be favorable energetically, which just caters for the observations at Figure 29b, 31b and 33. The intensity of π→π* is strong around 274 nm and even stronger than ICT.

The data from Table 2 shows that the maximum absorption of ICT processes is at 443 nm, and molar absorptivity is 35465 $M^{-1}cm^{-1}$ in dichloromethane and 43774 $M^{-1}cm^{-1}$ in acetonitrile. While the molar absorptivity in the mixture of acetonitrile and hypophosphorous acid is only 5422 $M^{-1}cm^{-1}$.

With the increase of polarity of solvents, a small redshift was observed on both phosphonium and phosphine oxide because of the stabilization of its ground state. The more polar solvent has a larger dipole moment, which can interact effectively with cation and neutral molecules to reach a stabilized ground state. Then the energy levels

decreased and energy gaps between the ground state and the excited state becomes larger.

8.2.2.Effects of protonation

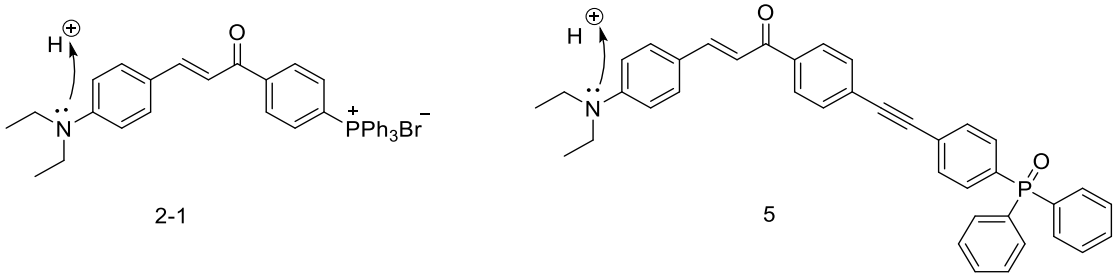

Scheme 8 *Protonating of* ***2-1*** *and* ***5*** *in the mixture of acetonitrile and hypophosphorous acid solution.*

When strong acid was added, the ICT process was suppressed. The lone pair electrons on nitrogen interact with a proton (Scheme 9). Electrons donate to the formation of hydrogen bonds rather than transit to high energy levels induced by light, then the capacity of electron transfer from it to cation center was weakened dramatically, which is reflected by the spectra in Figures 32 and 33, the molar absorptivity on ICT is only 5028 $M^{-1}cm^{-1}$. Non-protic acetonitrile only has dipole moment interactions with solvent dipole moments, while there is a combination of dipole moment interactions and hydrogen bonding interactions when protic hypophosphorous acid was mixed with acetonitrile.

The protonation breaks intramolecular charge transfer, the electrons are excited locally, which contributes to the strong absorption at a wavelength at 308 nm, the molar absorptivity is 15419 $M^{-1}cm^{-1}$ comparable to ICT in dichloromethane.

In the presence of protic acid, the hydrogen bonds could be formed, which contributes to the breaking of intramolecular charge transfer to the acceptor group of **5** because of the contribution of electrons on donor motif to hydrogen ions.

8.3. Emission Spectra

The distinct molecular structures of these compounds result in different emission after excitation. The emission spectra of **2-1**, **2-3**, **3**, **5** and **6** in CH_3CN at 293K was shown in Figure 34. The distinct molecular structure of these compounds results in different emissions.

Substitution of the counterions in compounds **2-1**, **2-2, 2-3** results in minor changes of emission spectra in solution of dichloromethane. Compound **6** has longer conjugation systems and different absorption wavelengths than compound **2-1**, but close emission

wavelengths for **2-1** and **6**, 562 nm and 558 nm, respectively. While for control group **3** and **5**, the emission wavelength is totally different even though they have same conjugation system just like **2-1** and **6**, the main difference is the acceptor, when the acceptor is a strong electron-withdrawing cation, then shorter wavelength of light will be emitted rather than at 600 nm for neutral acceptor. It is also the case for phosphonium **6**, 558 nm and phosphine oxide **5**, 616 nm.

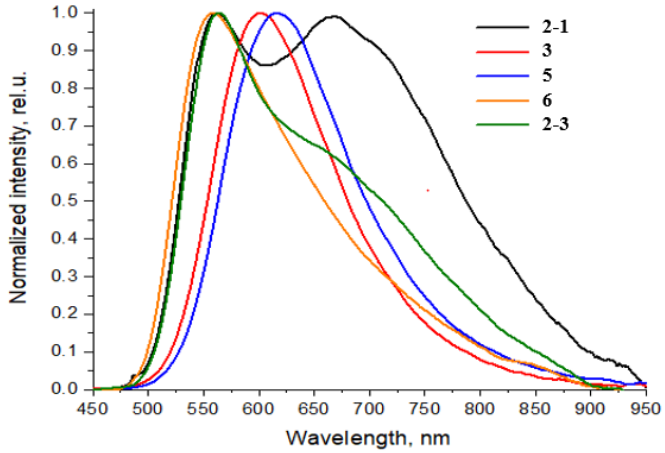

Figure 34 *Emission spectra of* ***2-1, 2-3, 3, 5, 6*** *in CH_3CN at 293K (excitation wavelength 365 nm).*

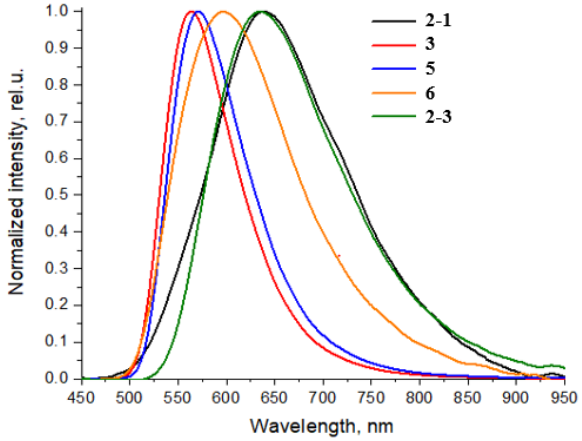

Figure 35 *Emission spectra of* ***2-1, 2-3, 3, 5, 6*** *in CH_2Cl_2 at 293K (excitation wavelength 365 nm).*

In less polar dichloromethane (Figure 35), there is no dual emission and each peak is separated independently. The emissive wavelength of **3** and **5** is still close to each other, but there is a huge extinction between **2-1** and **6**, the emission wavelength of **2-1**, 638 nm is longer than **6**, 596 nm in dichloromethane, rather than approximate equal in acetonitrile. Emission of salts **2-1** and **2-3** has the longest wavelength of 638 nm on **2-1** and 635 nm on **2-3**.

8.4. Solid State Emission Spectra

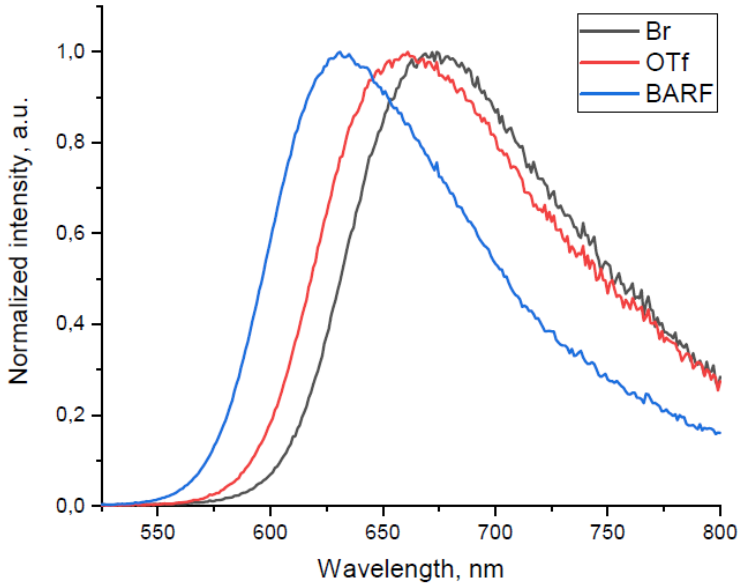

Figure 36 *The emission spectra of solid state* ***2-1, 2-2*** *and* ***2-3.***

The emission spectra of **2-1, 2-2** and **2-3** in solid state demonstrate counterion effects (Figure 36). They have the same conjugation lengths and electron donors, but different anions Br-, OTf, and BARF-. The differences in the emission maxima may be caused by cation-cation interaction. With the smaller anions connected to cations, the interactions between neighboring cations could be stronger due to the closer intermolecular distance, which affects the optical bandgap. Stronger interactions lead to a narrower energy gap, emitting low-energy emission light.

9. Conclusion

In conclusion, explorations have been conducted by constructing chalcone-based chromophores functionalized with phosphorus electron acceptors. Synthesis of these exclusive structures, characterization of their photophysical properties, dedicated to the absorption spectra of ICT processes and emission spectra, were carried out. Their structures were identified through ^{1}H NMR, together with XRD, mass spectrometry and elemental analysis. Different synthesis pathways were tested in order to get the highest yields. Intramolecular charge transfer processes were investigated among a series of synthesized phosphonium and phosphine oxides. The failure of synthesis of compounds **8**, **9** and **10** made the comparison of donor effects and conjugation effects on ICT process unattainable.

The comparison of length of conjugation (**2-1→6** and **3→5**), counterions (**2-1**, **2-2**, **2-3**), the variation of acceptors (**2-1→4**, **5→6)**, solvent polarity and acidity have

influences on the absorption and emission shape, intensity and position by distributing electron densities. The absorption of the studied phosphonium salts and phosphine oxides was tested in chloroform, emission was tested at dichloromethane and acetonitrile as well as in solid state. Highly feasible strong ICT processes were observed at different polarity solvents of dichloromethane and acetonitrile, but a low intensity on absorption was observed at an acidic mixture of acetonitrile and hypophosphorous acid.

Photophysical behaviors of synthesized phosphonium and phosphine oxides were influenced by the interaction of solvent, solvent polarity, donor and acceptor properties, conjugation length and solvent acidity.

10. Experimental Section

Synthesis of 1: A solution of 4-(diethylamino)benzaldehyde(1.8 g, 12.12 mmol) and 4'-bromoacetophenone (2.0 g, 10.10 mmol) in methanol (20 mL) was cooled to 0 °C. A solution of ethanol and KOH (2.5M, 30 mL) was added dropwise by using an addition funnel and stirring the reaction mixture at room temperature for 15 h. The product, precipitated as a dark-yellow solid, was filtered and washed with cold ethanol, yield 3.06 g (85%). ^{1}H NMR (400 MHz, $CDCl_3$): δ = 7.97 (d, *J* = 8.4 Hz, 2H), 7.89 (d, *J* = 15.2 Hz, 1H), 7.72 (d, *J* = 8.4 Hz, 2H), 7.63 (d, *J* = 8.8 Hz, 2H), 7.35 (d, *J* = 15.2 Hz, 1H), 6.76 (d, *J* =8.8 Hz, 2H), 3.53 (q, *J* = 7.2 Hz, 4H), 1.31 (t, *J* = 7.2 Hz, 6H).

Synthesis of 2-1: A solution of 1-(4-bromophenyl)-3-[4-(diethylamino)phenyl]-2-propen-1-one (198 mg, 0.59mmol), triphenylphosphine (154 mg, 0.59mmol) as well as catalyst $NiBr_2$ (20% mol, 25 mg) were added to ethylene glycol (3 mL) in a pressure vessel. The reaction mixture was flushed with nitrogen to 190 °C and stirred for 15 h. The reaction mixture turned into a deep yellow solution. After cooling down to room temperature, ethylene glycol was diluted with water three times (20 ml) and washed with dichloromethane three times (40 ml). The organic phase was collected, and dichloromethane was evaporated. The obtained crude product was purified by column chromatography (Silica gel 70-230 mesh, ⌀3.6×20 cm, eluent CH_2Cl_2/CH_3OH, 20/1) to give yellow powder, yield 0.28g (77%). ESI-MS (M/Z): $[M]^+$ 540.2438 (calcd 540.25). ^{1}H NMR (400 MHz, $CDCl_3$): δ = 8.34 (dd, *J* = 2.8 Hz, 2H), 8.01-7.64 (m, 12H), 7.79 (d, *J* = 2.8 Hz, 2H), 7.60 (d, *J* = 7.2 Hz, 2H), 7.35 (d, *J* = 12.4 Hz, 1H), 6.65 (d, *J* = 7.2 Hz, 2H), 3.47 (q, *J* = 6 Hz, 4H), 1.25 (t, *J* = 5.6 Hz, 6H). ^{31}P (162 MHz, $CDCl_3$): δ = 22.52 (s, 1P). Anal. Calcd for $C_{37}H_{35}BrNOP$: C, 71.71; H, 5.70; N, 2.26. Found: C, 70.41; H, 5.81; N, 2.21.

Synthesis of 2-2: Ion exchange of bromide ion to totetrakis[3,5-bis(trifluoromethyl)phenyl]borate ion ($BARF^-$) of **2-1**. Adding NaBARF (283mg, 0.32mmol) to 10 mL of diethyl ether, then **2-1** (200 mg, 0.32 mmol) was added to the solution, stirred for 1.5 h. Then filtering the white powder off and evaporation of the solution gave dark red solid. A TLC spot test confirmed the completeness of anion

exchange. Using column chromatography to purify the residue (Silica gel 70-230 mesh, ⌀3.6×20 cm, eluent CH_2Cl_2/CH_3OH, 20/1) to give dark red solid (489 mg, 95 %). ESI-MS (M/Z): $[M]^-$ 863.0883 (calcd 863.211). ^1H NMR (400 MHz, $CDCl_3$): δ = 8.39 (dd, *J* = 10 Hz, 1H), 8.01-7.64 (m), 7.41 (d, *J* = 4 Hz, 1H), 7.22 (d, *J* = 8 Hz, 2H), 3.47 (q, *J* = 7.2 Hz, 4H), 1.25 (t, *J* = 7.2 Hz, 6H). ^{31}P (162 MHz, $CDCl_3$): δ = 22.5 (s, 1P). Anal. Calcd for $C_{69}H_{47}NOPBF_{24}$: C, 59.03; H, 3.37; N, 1.00. Found: C, 59.25; H, 3.59; N, 0.95.

Synthesis of 2-3: Ion exchange of bromide ion to trifluoromethanesulfonate ion (OTf^-) of **2-1**. Adding NaOTf (55.05mg, 0.32mmol) to 10 mL of diethyl ether, then **2-1** (200 mg, 0.32 mmol) was added to the solution, stirred for 1.5 h. Then filtering the white powder off and evaporation of the solution gave to slight dark red solid. A TLC spot test confirmed the completeness of anion exchange. The residue was purified by column chromatography (Silica gel 70-230 mesh, ⌀3.6×20 cm, eluent CH_2Cl_2/CH_3OH, 20/1) to give slight dark red solid (176 mg, 80 %). ESI-MS (M/Z): $[M]^-$, 148.9541 (calcd 149.070). Anal. Calcd for $C_{38}H_{35}F_3NO_4PS$: C, 66.16; H, 5.13; N, 2.03; S, 4.65. Found: C, 66.11; H, 5.34; N, 2.07; S, 4.43.

Synthesis of 3: 4-bromoacetophenone (244 mg, 1.00 mmol), tetrakis(triphenylphosphine)palladium (60mg, 5% mol) were added to a two-neck round-bottom flask, the flask was vacuumed and connected to nitrogen to protect the catalyst and to provide an inert environment. Toluene (5 mL) and triethylamine (1 mL) and were added using a syringe under a nitrogen atmosphere. Finally, diphenylphosphine (186 mg, 1.00 mmol) was added to the system. The reaction system was stirred at 80 °C for 16 h. The system should be kept strictly in the nitrogen environment to avoid oxidation of the catalyst and diphenylphosphine. The reaction mixture appeared as a dark yellow solution. After cooling down to room temperature, toluene and triethylamine were removed under reduced pressure. Then a fast column chromatography (Silica gel 70-230 mesh, ⌀ 3×30 cm, eluent CH_2Cl_2/CH_3CH_3, 2/1) was conducted to get pure 4-(diphenylphosphino)acetophenone, white solid, yield, 182.60 mg (60%). ^1H NMR (400 MHz, $CDCl_3$): δ = 7.80 (d, *J* = 7.2 Hz, 2H), 7.35 - 7.15 (m, 12H), 2.50 (s, 3H). ^{31}P NMR (162 MHz, $CDCl_3$): δ = 20.82 (s, 1P).

Then the second-step condensation reaction between 4-(diphenylphosphino)acetophenone and 4-(diethylamino)benzaldehyde started. A solution of 4-(diphenylphosphino)acetophenone (200 mg, 0.66 mmol) and 4-(diethylamino)benzaldehyde (117 mg, 0.66mmol) in methanol (20 mL) was cooled to 0 °C under nitrogen atmosphere. A solution of ethanol and KOH (2.5M, 30 mL) was added dropwise by using an additional funnel and the reaction mixture was stirred at room temperature for 15 h. The solvents methanol and ethanol were removed by connecting the flask to reduced pressure. Then the third step was to oxidize the phosphorus-containing part with hydrogen peroxide. Adding 5 drops of hydrogen peroxide to dichloromethane solution of residual solid to get phosphorus oxides. Finally, the obtained crude product was purified by column chromatography (Silica gel 70-230

mesh, ⌀1.7×30 cm, eluent CH_2Cl_2/CH_3OH, 10/1) to give phosphorus oxide, yellow solid, yield 305.8 mg (68%). IR KBr; ν(C=O), 1716 cm^{-1}; ν(C=C), 1650 cm^{-1}. ESI-MS (M/Z): $[M]^+$ 480.2078 (calcd 480.21). ^1H NMR (400 MHz, $CDCl_3$): δ = 8.10 (d, *J* = 8.0 Hz, 2H), 7.90 (d, *J* = 15.6 Hz, 1H) 7.92-7.57 (m, 14H), 7.37 (d, *J* = 15.6 Hz, 1H), 6.76 (d, *J* = 8.8 Hz, 2H), 1.307 (t, *J* = 7.2 Hz, 6H). ^{31}P NMR (162 MHz, Acetone): δ = 28.81 (s, 1P). Anal. Calcd for $C_{31}H_{30}NO_2P$: C, 77.63; H, 6.32; N, 2.92. Found: C, 76.72; H, 6.25; N, 2.93.

Synthesis of 4: 1-(4-Bromophenyl)-3-[4-(diethylamino)phenyl]-2-propen-1-one (200 mg, 0.56mmol), 1-Bromo-4-ethynylbenzene (101 mg, 0.56mmol) and $Pd(PPh_3)Cl_2$ (39.3 mg, 0.028mmol) were added to a solution mixture of ethylenediamine (10 mL) and tetrahydrofuran (10 mL) under the nitrogen protection, The reaction mixture was stirred for 15 h, and then the solvent was removed under a reduced pressure. The residue was abstracted by water and dichloromethane and then purified by silica gel chromatography to afford a yellow powder of mid-product, yield 256 mg (64%). ^1H NMR (400 Hz, $CDCl_3$): δ = 8.10 (d, *J* = 8.4Hz, 2H), 7.90 (d, *J* = 15.2Hz, 1H), 7.72 (d, *J* = 8.4Hz, 2H), 7.64 (d, *J* = 8.8Hz, 2H), 7.61 (d, *J* = 8.4Hz, 2H), 7.52 (d, *J* = 8.4Hz, 2H), 7.41 (d, *J* = 15.2Hz, 2H), 6.77 (d, *J* = 8.4Hz, 2H), 3.53 (d, J_1 = 14.4Hz, J_2 = 7.2Hz, 4H), 1.32 (T, *J* = 7.2Hz, 6H).

Synthesis of 5: 4-iodo-bromobenzene (5.0 g, 17.68 mmol) was dissolved in an anhydrous triethylamine solution (20 mL) at room temperature. This solution was cooled in an ice bath, and $PdCl_2(PPh_3)_2$ (124 mg, 0.17 mmol) and CuI (34 mg, 0.17 mmol) were added. Cold trimethylsilylacetylene solution (1.74g, 17.68 mmol) was then added drop by drop. The mixture was stirred in an ice bath for 1.5 h, then the solvents were removed under reduced pressure and the residual solid was suspend in hexane. Passed the cruse product through a short silica column (eluent: hexanes) and concentrated the combined filtrates to obtain a colorless oil. The last step is to solidify the oil on drying in vacuum to obtain 4-(trimethylsilylethynyl)bromo benzene, yield 5.38 g (85%). ^1H NMR (400 MHz, $CDCl_3$): δ = 7.45–7.41 (m, 2H), 7.33–7.30 (m, 2H), 0.25 (s, 9H). Then to synthesize diphenyl-[4-trimethylsilylethynyl)phenyl]phosphane. To an anhydrous THF solution (40 mL), 4-bromo-(trimethylsilylethynyl)benzene (2.53 g, 9.3 mmol) was dissolved, when temperature was maintained at -78°C to -75 °C, *n*-BuLi (2.5 M, 3.1 mL) was added under nitrogen atmosphere. After 2h stirring, chlorodiphenylphosphine (2.53 g, 9.3 mmol) then was added. Additional 2h needed for stirring. Finally, the solvent was removed by rotary evaporator under a reduced pressure. Using silica gel chromatography to purify the residue, a white powder was got, yield 2.00 g (60%). ^1H NMR ($CDCl_3$): δ = 7.42–7.16 (m, 14H), 0.22 (s, 9H). ^{31}P ($CDCl_3$): δ = - 5.75 (s, 1P).

The next step is to prepare of Ph2P-Ph-C ≡ CH.[117] To a methanol (50 mL) and dichloromethane (10 mL) solution of Ph_2P-Ph-≡-$SiMe_3$ (1.63 g, 4.55 mmol), was added K_2CO_3 (1.26 g, 9.09 mmol). The suspension was stirred at room temperature for 2 h and was then filtered. The crude product was purified by silica gel chromatography to

give 4-(Ethynylphenyl)diphenylphosphine, white solid, yield 1.10 g (85%). ^{1}H NMR (400 MHz, $CDCl_3$): σ 7.48–7.20 (m, 14H), 3.11 (s, 1H). ^{31}P NMR (162 MHz, $CDCl_3$): δ = - 5.74 (s). The third step is to get (4-Ethynylphenyl)diphenylphosphine oxide. Diphenyl-[4-trimethylsilylethynyl)phenyl]phosphane (0.5 g, 1.1 mmol) was dissolved in a mixture of dichloromethane (30 mL) and methanol (30 mL), then hydrogen peroxide (30% solution, 1.7 mL) was added slowly. Stirring 2h for the resulting mixture, then aqueous Na_2SO_3 solution was added to quench it and extracted with dichloromethane. $MgSO_4$ was used to dry the combined organic phases, then filtered, and concentrated under reduced pressure to give a white solid, yield 0.5 g (96%). ^{1}H NMR (400 MHz, $CDCl_3$): δ = 7.45–7.38 (m, 10H), 7.43–7.40 (m, 4H), 3.24 (s, 1H). ^{31}P NMR (162 MHz, $CDCl_3$): δ = 28.7 (s, 1P).

Finally, (4-Ethynylphenyl)diphenylphosphine oxide (248 mg, 0.82mmol), 1-(4-Bromophenyl)-3-[4-(diethylamino)phenyl]-2-propen-1-one (294.5 mg, 0.82mmol), and $Pd(PPh_3)Cl_2$ (57.5 mg, 10%mmol) were added to a mixed solution of tetrahydrofuran (10 mL) and ethylenediamine (10 mL), then CuI (15.6mg, 10%mmol) was added before nitrogen protection of reacting conditions. It took 15 h at room temperature. The organic phase was collected, and the residue was purified by column chromatography (Silica gel 70-230 mesh, ⌀3.6×20 cm, eluent CH_2Cl_2/CH_3OH, 10/1) to give dark red solid (356 mg, 75%). ^{1}H NMR (400 MHz, CHCl3): δ = 8.10 (d, J = 8.4Hz, 2H), 7.90 (d, J = 15.6Hz, 2H) 7.80-7.59 (m, 20H), 7.37 (d, J = 6Hz, 1H), 6.76 (d, J = 8.8Hz, 2H), 3.52(q, J_1 = 14.8Hz, J_2 = 7.2Hz 4H), 1.31 (t, J = 6.8Hz 6H). ^{31}P NMR (162 MHz, $CDCl_3$): δ = 28.34 (s, 1P). Anal. Calcd for $C_{33}H_{30}NO_2P$: C, 78.70; H, 6.02; N, 2.78. Found: C, 78.93; H, 5.94; N, 2.17.

Synthesis of 6: **4** (200 mg, 0.43 mmol) reacted with triphenylphosphine (113 mg, 0.43 mmol) under the presence of $Pd(dba)_2$ (4 mg, 1% mmol) in toluene (4 mL) at 130 °C for 15 h. toluene was removed by rotary evaporator under a reduced pressure. The solid product was abstracted by water and dichloromethane and then purified by silica gel chromatography to afford a yellow powder of phosphonium, yield 182.8 mg (59%) ^{1}H NMR (400Hz, $CDCl_3$): δ = 8.09 (d, J = 8.4Hz, 2H), 8.03–7.73 (m, 21H), 7.63 (d, J = 8.8Hz, 2H), 3.52 (q, J_1 = 14.2Hz, J_2 = 7.2Hz, 4H), 1.30 (t, J = 7.2Hz, 6H). ^{31}P NMR (162 MHz, $CDCl_3$): δ = 22.62 (s, 1P). Anal. Calcd for $C_{39}H_{35}BrNOP$: C, 72.76; H, 5.50; N, 2.18. Found: C, 73.67; H, 5.56; N, 1.93.

11. References

(1) Barbara, P. F.; Walker, G. C.; Smith, T. P. Vibrational Modes and the Dynamic Solvent Effect in Electron and Proton Transfer. *Science (80-.).* **1992**, *256* (5059), 975–981. https://doi.org/10.1126/science.256.5059.975.

(2) Closs, G. L.; Miller, J. R. Intramolecular Long-Distance Electron Transfer in Organic Molecules The Basic Models and the Foundation of Their LTheoretical Description. *Science (80-.).* **1988**, *240*, 440–447.

(3) Calbert, J. P.; Filho, D. A. S.; Cornil, J.; Bre, J. L. Proceedings of the National Academy of Sciences_2002_Brédas_Organic Semiconductors A Theoretical Characterization of the Basic Parameters Governing Charge Transport-1.Pdf. **2002**, *99* (9).

(4) Bulheller, B. M.; Miles, A. J.; Wallace, B. A.; Hirst, J. D. Charge-Transfer Transitions in the Vacuum-Ultraviolet of Protein Circular Dichroism Spectra. *J. Phys. Chem. B* **2008**, *112* (6), 1866–1874. https://doi.org/10.1021/jp077462k.

(5) Kobori, Y.; Yamauchi, S.; Akiyama, K.; Tero-Kubota, S.; Imahori, H.; Fukuzumi, S.; Norris, J. R. Primary Charge-Recombination in an Artificial Photosynthetic Reaction Center. *Proc. Natl. Acad. Sci.* **2005**, *102* (29), 10017–10022. https://doi.org/10.1073/pnas.0504598102.

(6) Zhao, G. J.; Liu, J. Y.; Zhou, L. C.; Han, K. L. Site-Selective Photoinduced Electron Transfer from Alcoholic Solvents to the Chromophore Facilitated by Hydrogen Bonding: A New Fluorescence Quenching Mechanism. *J. Phys. Chem. B* **2007**, *111* (30), 8940–8945. https://doi.org/10.1021/jp0734530.

(7) Cortés-Arriagada, D.; Cárdenas-Jirón, G. I. A Through-Space Charge Transfer Mechanism for Explaining the Oxidation of 2-Chlorophenol on a Tetrasulphonated Nickel(III) Phthalocyanine. *Comput. Theor. Chem.* **2011**, *963* (1), 161–167. https://doi.org/10.1016/j.comptc.2010.10.015.

(8) RamprasadMisraandS.P.Bhattacharyya. An Overview of the ICT Process. In *Intramolecular Charge Transfer: Theory and Applications*; 2018; p 14.

(9) Chris P Schaller, P. D. ； Ji. C. Electronic Spectroscopy.

(10) Beinhoff, M.; Modrakowski, C.; Brüdgam, I.; Hartl, H.; Schlüter, A. D.; Weigel, W.; Jurczok, M.; Rettig, W. Synthesis and Spectroscopic Properties of Arene-Substituted Pyrene Derivatives as Model Compounds for Fluorescent Polarity Probes. *European J. Org. Chem.* **2001**, *49* (20), 3819–3829. https://doi.org/10.1002/1099-0690(200110)2001:203.0.CO;2-W.

(11) Beinhoff, M.; Weigel, W.; Rettig, W.; Bruedgam, I.; Hartl, H.; Schlueter, A. D. Phenylene Alkylene Dendrons with Site-Specific Incorporated Fluorescent Pyrene Probes. *J. Org. Chem.* **2005**, *70* (17), 6583–6591. https://doi.org/10.1021/jo050302p.

(12) Techert, S.; Wiessner, A.; Schmatz, S.; Staerk, H. Time-Resolved Fluorescence and Solvatochromy of Directly Linked Pyrene-DMA Derivatives in Alcoholic Solution. *J. Phys. Chem. B* **2001**, *105* (31), 7579–7587. https://doi.org/10.1021/jp004370l.

(13) Zayed, M. E. M.; El-Shishtawy, R. M.; Elroby, S. A.; Al-Footy, K. O.; Al-amshany, Z. M. Experimental and Theoretical Study of Donor-π-Acceptor Compounds Based on Malononitrile. *Chem. Cent. J.* **2018**, *12* (1), 1–10. https://doi.org/10.1186/s13065-018-0394-5.

(14) Druzhinin, S. I.; Zachariasse, K. A.; Mayer, P.; Stalke, D.; Von Bülow, R.; Noltemeyer, M. Intramolecular Charge Transfer with 1-Tert-Butyl-6-Cyano-1,2,3,4- Tetrahydroquinoline (NTC6) and Other Aminobenzonitriles. A Comparison of Experimental Vapor Phase Spectra and Crystal Structures with Calculations. *J. Am. Chem. Soc.* **2010**, *132* (22), 7730–7744. https://doi.org/10.1021/ja101336n.

(15) Bhattacharyya, R. and S. P. *Introduction to Intramolecular Charge Transfer：theory and Applications*.

(16) Moyon, N. S.; Mitra, S. Fluorescence Solvatochromism in Lumichrome and Excited-State Tautomerization: A Combined Experimental and DFT Study. *J. Phys. Chem. A* **2011**, *115* (12), 2456–2464. https://doi.org/10.1021/jp1102687.

(17) Chen, Y.; Guo, J.; Wu, X.; Jia, D.; Tong, F. Color-Tuning Aggregation-Induced Emission of o-Carborane-Bis(1,3,5-Triaryl-2-Pyrazoline) Triads: Preparation and Investigation of the

Photophysics. *Dye. Pigment.* **2018**, *148*, 180–188. https://doi.org/10.1016/j.dyepig.2017.09.011.

(18) Vendrell, M.; Zhai, D.; Er, J. C.; Chang, Y. Chem. Rev 2012.Pdf. **2011**.

(19) Zaccheroni, N.; Palomba, F.; Rampazzo, E. Luminescent Chemosensors: From Molecules to Nanostructures. **2016**, 479–497. https://doi.org/10.1007/978-3-319-31671-0_12.

(20) Rhodamine - an overview | ScienceDirect Topics https://www.sciencedirect.com/topics/biochemistry-genetics-and-molecular-biology/rhodamine (accessed Apr 13, 2020).

(21) Panja, S. K.; Dwivedi, N.; Saha, S. Tuning the Intramolecular Charge Transfer (ICT) Process in Push-Pull Systems: Effect of Nitro Groups. *RSC Adv.* **2016**, *6* (107), 105786–105794. https://doi.org/10.1039/c6ra17521j.

(22) Joly, D.; Bouit, P. A.; Hissler, M. Organophosphorus Derivatives for Electronic Devices. *Journal of Materials Chemistry C*. Royal Society of Chemistry 2016, pp 3686–3698. https://doi.org/10.1039/c6tc00590j.

(23) Suhr Kirketerp, M.-B.; Åxman Petersen, M.; Wanko, M.; Andres Espinosa Leal, L.; Zettergren, H.; Raymo, F. M.; Rubio, A.; Brøndsted Nielsen, M.; Brøndsted Nielsen, S. Absorption Spectra of 4-Nitrophenolate Ions Measured *in Vacuo* and in Solution. *ChemPhysChem* **2009**, *10* (8), 1207–1209. https://doi.org/10.1002/cphc.200900174.

(24) El-Dossoki, F. I.; Abdallh, N. E. Y.; Elmasly, S. E. T. The Transport Properties and the Association Behavior of Some 1:1 and 2:1 Electrolytes in Some Binary Alcoholic-Aqueous Mixtures. *J. Mol. Liq.* **2011**, *163* (3), 135–140. https://doi.org/10.1016/j.molliq.2011.08.009.

(25) Panja, S. K.; Dwivedi, N.; Saha, S. Tuning the Intramolecular Charge Transfer (ICT) Process in Push-Pull Systems: Effect of Nitro Groups. *RSC Adv.* **2016**, *6* (107), 105786–105794. https://doi.org/10.1039/c6ra17521j.

(26) Lin, M. S.; Yang, S. J.; Chang, H. W.; Huang, Y. H.; Tsai, Y. T.; Wu, C. C.; Chou, S. H.; Mondal, E.; Wong, K. T. Incorporation of a CN Group into MCP: A New Bipolar Host Material for Highly Efficient Blue and White Electrophosphorescent Devices. *J. Mater. Chem.* **2012**, *22* (31), 16114–16120. https://doi.org/10.1039/c2jm32717a.

(27) Li, W.; Li, J.; Liu, D.; Li, D.; Zhang, D. Dual N-Type Units Including Pyridine and Diphenylphosphine Oxide: Effective Design Strategy of Host Materials for High-Performance Organic Light-Emitting Diodes. *Chem. Sci.* **2016**, *7* (11), 6706–6714. https://doi.org/10.1039/c6sc01797e.

(28) Justin Thomas, K. R.; Velusamy, M.; Lin, J. T.; Tao, Y.-T.; Chuen, C.-H. Cyanocarbazole Derivatives for High-Performance Electroluminescent Devices. *Adv. Funct. Mater.* **2004**, *14* (4), 387–392. https://doi.org/10.1002/adfm.200305144.

(29) Lin, M. S.; Yang, S. J.; Chang, H. W.; Huang, Y. H.; Tsai, Y. T.; Wu, C. C.; Chou, S. H.; Mondal, E.; Wong, K. T. Incorporation of a CN Group into MCP: A New Bipolar Host Material for Highly Efficient Blue and White Electrophosphorescent Devices. *J. Mater. Chem.* **2012**, *22* (31), 16114–16120. https://doi.org/10.1039/c2jm32717a.

(30) Gudeika, D.; Grazulevicius, J. V.; Volyniuk, D.; Juska, G.; Jankauskas, V.; Sini, G. Effect of Ethynyl Linkages on the Properties of the Derivatives of Triphenylamine and 1,8-Naphthalimide. *J. Phys. Chem. C* **2015**, *119* (51), 28335–28346. https://doi.org/10.1021/acs.jpcc.5b10163.

(31) Kato, S. I.; Noguchi, H.; Kobayashi, A.; Yoshihara, T.; Tobita, S.; Nakamura, Y. Bicarbazoles:

Systematic Structure-Property Investigations on a Series of Conjugated Carbazole Dimers. *J. Org. Chem.* **2012**, *77* (20), 9120–9133. https://doi.org/10.1021/jo3016538.

(32) Gierschner, J.; Park, S. Y. Luminescent Distyrylbenzenes: Tailoring Molecular Structure and Crystalline Morphology. *J. Mater. Chem. C* **2013**, *1* (37), 5818–5832. https://doi.org/10.1039/c3tc31062k.

(33) Shimizu, M.; Hiyama, T. Organic Fluorophores Exhibiting Highly Efficient Photoluminescence in the Solid State. *Chem. - An Asian J.* **2010**, *5* (7), 1516–1531. https://doi.org/10.1002/asia.200900727.

(34) Hinoue, T.; Shigenoi, Y.; Sugino, M.; Mizobe, Y.; Hisaki, I.; Miyata, M.; Tohnai, N. Regulation of π-Stacked Anthracene Arrangement for Fluorescence Modulation of Organic Solid from Monomer to Excited Oligomer Emission. *Chem. - A Eur. J.* **2012**, *18* (15), 4634–4643. https://doi.org/10.1002/chem.201103518.

(35) Shi, J.; Aguilar Suarez, L. E.; Yoon, S. J.; Varghese, S.; Serpa, C.; Park, S. Y.; Lüer, L.; Roca-Sanjuán, D.; Milián-Medina, B.; Gierschner, J. Solid State Luminescence Enhancement in π-Conjugated Materials: Unraveling the Mechanism beyond the Framework of AIE/AIEE. *J. Phys. Chem. C* **2017**, *121* (41), 23166–23183. https://doi.org/10.1021/acs.jpcc.7b08060.

(36) Liang, J.; Tang, B. Z.; Liu, B. Specific Light-up Bioprobes Based on AIEgen Conjugates. *Chem. Soc. Rev.* **2015**, *44* (10), 2798–2811. https://doi.org/10.1039/c4cs00444b.

(37) Luo, J.; Xie, Z.; Xie, Z.; Lam, J. W. Y.; Cheng, L.; Chen, H.; Qiu, C.; Kwok, H. S.; Zhan, X.; Liu, Y.; et al. Aggregation-Induced Emission of 1-Methyl-1,2,3,4,5-Pentaphenylsilole. *Chem. Commun.* **2001**, *18*, 1740–1741. https://doi.org/10.1039/b105159h.

(38) Huang, M.; Yu, R.; Xu, K.; Ye, S.; Kuang, S.; Zhu, X.; Wan, Y. An Arch-Bridge-Type Fluorophore for Bridging the Gap between Aggregation-Caused Quenching (ACQ) and Aggregation-Induced Emission (AIE). *Chem. Sci.* **2016**, *7* (7), 4485–4491. https://doi.org/10.1039/c6sc01254j.

(39) Hirose, T.; Matsuda, K. Self-Assembly of Amphiphilic Fluorescent Dyes Showing Aggregate-Induced Enhanced Emission: Temperature Dependence of Molecular Alignment and Intermolecular Interaction in Aqueous Environment. *Chem. Commun.* **2009**, No. 39, 5832–5834. https://doi.org/10.1039/b910531j.

(40) Nishio, S.; Higashiguchi, K.; Matsuda, K. The Effect of Cyano Substitution on the Fluorescence Behavior of 1,2-Bis(Pyridylphenyl)Ethene. *Asian J. Org. Chem.* **2014**, *3* (6), 686–690. https://doi.org/10.1002/ajoc.201402024.

(41) Nishio, S.; Higashiguchi, K.; Matsuda, K. The Effect of Cyano Substitution on the Fluorescence Behavior of 1,2-Bis(Pyridylphenyl)Ethene. *Asian J. Org. Chem.* **2014**, *3* (6), 686–690. https://doi.org/10.1002/ajoc.201402024.

(42) Oelkrug, D.; Tompert, A.; Egelhaaf, H. J.; Hanack, M.; Steinhuber, E.; Hohloch, M.; Meier, H.; Stalmach, U. Towards Highly Luminescent Phenylene Vinylene Films. *Synth. Met.* **1996**, *83* (3), 231–237. https://doi.org/10.1016/S0379-6779(96)04484-0.

(43) Pahlavanlu, P.; Christensen, P. R.; Therrien, J. A.; Wolf, M. O. Controlled Intramolecular Charge Transfer Using a Sulfur-Containing Acceptor Group. *J. Phys. Chem. C* **2016**, *120* (1), 70–77. https://doi.org/10.1021/acs.jpcc.5b09826.

(44) Christensen, P. R.; Nagle, J. K.; Bhatti, A.; Wolf, M. O. Enhanced Photoluminescence of Sulfur-Bridged Organic Chromophores. *J. Am. Chem. Soc.* **2013**, *135* (22), 8109–8112. https://doi.org/10.1021/ja401383q.

(45) Dell, E. J.; Campos, L. M. The Preparation of Thiophene-S,S-Dioxides and Their Role in Organic Electronics. *J. Mater. Chem.* **2012**, *22* (26), 12945–12952. https://doi.org/10.1039/c2jm31220d.

(46) Camaioni, N.; Ridolfi, G.; Fattori, V.; Favaretto, L.; Barbarella, G. Oligothiophene-S, S-Dioxides as a Class of Electron-Acceptor Materials for Organic Photovoltaics. *Appl. Phys. Lett.* **2004**, *84* (11), 1901–1903. https://doi.org/10.1063/1.1682681.

(47) Cui, C.; Wong, W. Y.; Li, Y. Improvement of Open-Circuit Voltage and Photovoltaic Properties of 2D-Conjugated Polymers by Alkylthio Substitution. *Energy Environ. Sci.* **2014**, *7* (7), 2276–2284. https://doi.org/10.1039/c4ee00446a.

(48) Tang, C. W. Two-Layer Organic Photovoltaic Cell. *Appl. Phys. Lett.* **1986**, *48* (2), 183–185. https://doi.org/10.1063/1.96937.

(49) Guo, C.; Lin, Y. H.; Witman, M. D.; Smith, K. A.; Wang, C.; Hexemer, A.; Strzalka, J.; Gomez, E. D.; Verduzco, R. Conjugated Block Copolymer Photovoltaics with near 3% Efficiency through Microphase Separation. *Nano Lett.* **2013**, *13* (6), 2957–2963. https://doi.org/10.1021/nl401420s.

(50) Lee, D. H.; Lee, J. H.; Kim, H. J.; Choi, S.; Park, G. E.; Cho, M. J.; Choi, D. H. (D)n-σ-(A)m Type Partially Conjugated Block Copolymer and Its Performance in Single-Component Polymer Solar Cells. *J. Mater. Chem. A* **2017**, *5* (20), 9745–9751. https://doi.org/10.1039/c7ta01819c.

(51) Roncali, J. Single Material Solar Cells: The next Frontier for Organic Photovoltaics? *Adv. Energy Mater.* **2011**, *1* (2), 147–160. https://doi.org/10.1002/aenm.201000008.

(52) Gierschner, J.; Lüer, L.; Milián-Medina, B.; Oelkrug, D.; Egelhaaf, H. J. Highly Emissive H-Aggregates or Aggregation-Induced Emission Quenching? The Photophysics of All-Trans Para-Distyrylbenzene. *Journal of Physical Chemistry Letters*. American Chemical Society August 15, 2013, pp 2686–2697. https://doi.org/10.1021/jz400985t.

(53) Doty, J. C.; Babb, B.; Grisdale, P. J.; Glogowski, M.; Williams, J. L. R. Boron Photochemistry. IX. Synthesis and Fluorescent Properties of Dimesityl-Phenylboranes. *J. Organomet. Chem.* **1972**, *38* (2), 229–236. https://doi.org/10.1016/S0022-328X(00)83321-5.

(54) Sudhakar, P.; Mukherjee, S.; Thilagar, P. Revisiting Borylanilines: Unique Solid-State Structures and Insight into Photophysical Properties. *Organometallics* **2013**, *32* (10), 3129–3133. https://doi.org/10.1021/om301197f.

(55) Li, F.; Jia, W.; Wang, S.; Zhao, Y.; Lu, Z. H. Blue Organic Light-Emitting Diodes Based on Mes2B [p-4, 4′ -Biphenyl-NPh(1-Naphthyl)]. *J. Appl. Phys.* **2008**, *103* (3), 034509. https://doi.org/10.1063/1.2841459.

(56) Sundararaman, A.; Varughese, R.; Li, H.; Zakharov, L. N.; Rheingold, A. L.; Jäkle, F. A Donor-Acceptor Dyad with a Highly Lewis Acidic Boryl Group. *Organometallics* **2007**, *26* (25), 6126–6131. https://doi.org/10.1021/om700520n.

(57) Wakamiya, A.; Mori, K.; Yamaguchi, S. 3-Boryl-2,2′-Bithiophene as a Versatile Core Skeleton for Full-Color Highly Emissive Organic Solids. *Angew. Chemie - Int. Ed.* **2007**, *46* (23), 4273–4276. https://doi.org/10.1002/anie.200604935.

(58) Regulska, E.; Hindenberg, P.; Romero-Nieto, C. From Phosphaphenalenes to Diphosphahexaarenes: An Overview of Linearly Fused Six-Membered Phosphorus Heterocycles. *Eur. J. Inorg. Chem.* **2019**, *2019* (11–12), 1519–1528. https://doi.org/10.1002/ejic.201801340.

(59) Fave, C.; Cho, T. Y.; Hissler, M.; Chen, C. W.; Luh, T. Y.; Wu, C. C.; Réau, R. First Examples of Organophosphorus-Containing Materials for Light-Emitting Diodes. *J. Am. Chem. Soc.* **2003**, *125* (31), 9254–9255. https://doi.org/10.1021/ja035155w.

(60) Öberg, E.; Orthaber, A.; Lescop, C.; Réau, R.; Hissler, M.; Ott, S. Phosphorus Centers of Different Hybridization in Phosphaalkene-Substituted Phospholes. *Chem. - A Eur. J.* **2014**, *20* (27), 8421–8432. https://doi.org/10.1002/chem.201402406.

(61) Nakabuchi, T.; Matano, Y.; Imahori, H. Remarkable Effects of P-Perfluorophenyl Group on the Synthesis of Core-Modified Phosphaporphyrinoids and Phosphadithiasapphyrin. *Org. Lett.* **2010**, *12* (5), 1112–1115. https://doi.org/10.1021/ol100114j.

(62) Zhou, Y.; Yang, S.; Li, J.; He, G.; Duan, Z.; Mathey, F. Phosphorus and Silicon-Bridged Stilbenes: Synthesis and Optoelectronic Properties. *Dalt. Trans.* **2016**, *45* (45), 18308–18312. https://doi.org/10.1039/c6dt03489f.

(63) Zhuang, Z.; Bu, F.; Luo, W.; Peng, H.; Chen, S.; Hu, R.; Qin, A.; Zhao, Z.; Tang, B. Z. Steric, Conjugation and Electronic Impacts on the Photoluminescence and Electroluminescence Properties of Luminogens Based on Phosphindole Oxide. *J. Mater. Chem. C* **2017**, *5* (7), 1836–1842. https://doi.org/10.1039/c6tc05591e.

(64) Zhou, X.; Lai, R.; Beck, J. R.; Li, H.; Stains, C. I. Nebraska Red: A Phosphinate-Based near-Infrared Fluorophore Scaffold for Chemical Biology Applications. *Chem. Commun.* **2016**, *52* (83), 12290–12293. https://doi.org/10.1039/c6cc05717a.

(65) Yamaguchi, E.; Fukazawa, A.; Kosaka, Y.; Yokogawa, D.; Irle, S.; Yamaguchi, S. A Benzophosphole P-Oxide with an Electron-Donating Group at 3-Position: Enhanced Fluorescence in Polar Solvents. *Bull. Chem. Soc. Jpn.* **2015**, *88* (11), 1545–1552. https://doi.org/10.1246/bcsj.20150238.

(66) Higashino, T.; Ishida, K.; Satoh, T.; Matano, Y.; Imahori, H. Phosphole-Thiophene Hybrid: A Dual Role of Dithieno[3,4- b:3′,4′- d] Phosphole as Electron Acceptor and Electron Donor. *J. Org. Chem.* **2018**, *83* (6), 3397–3402. https://doi.org/10.1021/acs.joc.8b00030.

(67) Yamaguchi, S.; Fukazawa, A.; Taki, M. Phosphole <I>P</I>-Oxide-Containing π-Electron Materials: Synthesis and Applications in Fluorescence Imaging. *J. Synth. Org. Chem. Japan* **2017**, *75* (11), 1179–1187. https://doi.org/10.5059/yukigoseikyokaishi.75.1179.

(68) Xu, Y.; Wang, Z.; Gan, Z.; Xi, Q.; Duan, Z.; Mathey, F. Versatile Synthesis of Phospholides from Open-Chain Precursors. Application to Annelated Pyrrole- and Silole-Phosphole Rings. *Org. Lett.* **2015**, *17* (7), 1732–1734. https://doi.org/10.1021/acs.orglett.5b00598.

(69) Allen, D. W. Phosphines and Related C-P Bonded Compounds. *Organophosphorus Chemistry*. Royal Society of Chemistry 2017, pp 1–51. https://doi.org/10.1039/9781788010689-00001.

(70) Lee, Y. H.; Jana, S.; Lee, H.; Lee, S. U.; Lee, M. H. Rational Design of Time-Resolved Turn-on Fluorescence Sensors: Exploiting Delayed Fluorescence for Hydrogen Peroxide Sensing. *Chem. Commun.* **2018**, *54* (85), 12069–12072. https://doi.org/10.1039/c8cc07397j.

(71) Jeon, S. O.; Lee, J. Y. Phosphine Oxide Derivatives for Organic Light Emitting Diodes. *J. Mater. Chem.* **2012**, *22* (10), 4233–4243. https://doi.org/10.1039/c1jm14832j.

(72) Lee, J.; Aizawa, N.; Yasuda, T. Molecular Engineering of Phosphacycle-Based Thermally Activated Delayed Fluorescence Materials for Deep-Blue OLEDs. *J. Mater. Chem. C* **2018**, *6* (14), 3578–3583. https://doi.org/10.1039/c7tc05709a.

(73) Baumgartner, T.; Neumann, T.; Wirges, B. The Dithieno[3,2-b:2′,3′-d]Phosphole System: A Novel Building Block for Highly Luminescent π-Conjugated Materials. *Angew. Chemie - Int.*

Ed. **2004**, *43* (45), 6197–6201. https://doi.org/10.1002/anie.200461301.

(74) Lee, J.; Aizawa, N.; Yasuda, T. Molecular Engineering of Phosphacycle-Based Thermally Activated Delayed Fluorescence Materials for Deep-Blue OLEDs. *J. Mater. Chem. C* **2018**, *6* (14), 3578–3583. https://doi.org/10.1039/c7tc05709a.

(75) Jeon, S. O.; Jang, S. E.; Son, H. S.; Lee, J. Y. External Quantum Efficiency Above 20% in Deep Blue Phosphorescent Organic Light-Emitting Diodes. *Adv. Mater.* **2011**, *23* (12), 1436–1441. https://doi.org/10.1002/adma.201004372.

(76) Chou, H. H.; Cheng, C. H. A Highly Efficient Universal Bipolar Host for Blue, Green, and Red Phosphorescent OLEDs. *Adv. Mater.* **2010**, *22* (22), 2468–2471. https://doi.org/10.1002/adma.201000061.

(77) Thiery, S.; Tondelier, D.; Geffroy, B.; Jacques, E.; Robin, M.; Métivier, R.; Jeannin, O.; Rault-Berthelot, J.; Poriel, C. Spirobifluorene-2,7-Dicarbazole-4′-Phosphine Oxide as Host for High-Performance Single-Layer Green Phosphorescent OLED Devices. *Org. Lett.* **2015**, *17* (19), 4682–4685. https://doi.org/10.1021/acs.orglett.5b02027.

(78) Shao, S.; Ding, J.; Ye, T.; Xie, Z.; Wang, L.; Jing, X.; Wang, F. A Novel, Bipolar Polymeric Host for Highly Efficient Blue Electrophosphorescence: A Non-Conjugated Poly(Aryl Ether) Containing Triphenylphosphine Oxide Units in the Electron-Transporting Main Chain and Carbazole Units in Hole-Transporting Side Chains. *Adv. Mater.* **2011**, *23* (31), 3570–3574. https://doi.org/10.1002/adma.201101074.

(79) Ho, K. W.; Ariffin, A. Synthesis, Photophysical, and Electrochemical Properties of Wide Band Gap Tetraphenylsilane-Carbazole Derivatives: Effect of the Substitution Position and Naphthalene Side Chain. *Russ. J. Phys. Chem. A* **2016**, *90* (13), 2590–2599. https://doi.org/10.1134/S0036024416130124.

(80) Chai, X.; Cui, X.; Wang, B.; Yang, F.; Cai, Y.; Wu, Q.; Wang, T. Near-Infrared Phosphorus-Substituted Rhodamine with Emission Wavelength above 700 Nm for Bioimaging. *Chem. - A Eur. J.* **2015**, *21* (47), 16754–16758. https://doi.org/10.1002/chem.201502921.

(81) Wang, C.; Fukazawa, A.; Taki, M.; Sato, Y.; Higashiyama, T.; Yamaguchi, S. A Phosphole Oxide Based Fluorescent Dye with Exceptional Resistance to Photobleaching: A Practical Tool for Continuous Imaging in STED Microscopy. *Angew. Chemie* **2015**, *127* (50), 15428–15432. https://doi.org/10.1002/ange.201507939.

(82) Zheng, Q.; Lavis, L. D. Development of Photostable Fluorophores for Molecular Imaging. *Current Opinion in Chemical Biology*. Elsevier Ltd August 1, 2017, pp 32–38. https://doi.org/10.1016/j.cbpa.2017.04.017.

(83) Wang, C.; Fukazawa, A.; Taki, M.; Sato, Y.; Higashiyama, T.; Yamaguchi, S. A Phosphole Oxide Based Fluorescent Dye with Exceptional Resistance to Photobleaching: A Practical Tool for Continuous Imaging in STED Microscopy. *Angew. Chemie - Int. Ed.* **2015**, *54* (50), 15213–15217. https://doi.org/10.1002/anie.201507939.

(84) Giordan, J. C.; Moore, J. H.; Tossell, J. A.; Kaim, W. Interaction of Frontier Orbitals of Group 15 and Group 16 Methides with the Frontier Orbitals of Benzene. *J. Am. Chem. Soc.* **1985**, *107* (20), 5600–5604. https://doi.org/10.1021/ja00306a003.

(85) Christianson, A. M.; Gabbaï, F. P. Synthesis and Coordination Chemistry of a Phosphine-Decorated Fluorescein: "Double Turn-On" Sensing of Gold(III) Ions in Water. *Inorg. Chem.* **2016**, *55* (12), 5828–5835. https://doi.org/10.1021/acs.inorgchem.6b00080.

(86) Bouit, P. A.; Escande, A.; Szücs, R.; Szieberth, D.; Lescop, C.; Nyulászi, L.; Hissler, M.; Réau,

R. Dibenzophosphapentaphenes: Exploiting P Chemistry for Gap Fine-Tuning and Coordination-Driven Assembly of Planar Polycyclic Aromatic Hydrocarbons. *J. Am. Chem. Soc.* **2012**, *134* (15), 6524–6527. https://doi.org/10.1021/ja300171y.

(87) Belyaev, A.; Cheng, Y.; Liu, Z.; Karttunen, A. J.; Chou, P.; Koshevoy, I. O. A Facile Molecular Machine: Optically Triggered Counterion Migration by Charge Transfer of Linear Donor-π-Acceptor Phosphonium Fluorophores. *Angew. Chemie Int. Ed.* **2019**, *58* (38), 13456–13465. https://doi.org/10.1002/anie.201906929.

(88) Shameem, M. A.; Orthaber, A. Organophosphorus Compounds in Organic Electronics. *Chem. - A Eur. J.* **2016**, *22* (31), 10718–10735. https://doi.org/10.1002/chem.201600005.

(89) Stolar, M.; Baumgartner, T. Phosphorus-Containing Materials for Organic Electronics. *Chem. - An Asian J.* **2014**, *9* (5), 1212–1225. https://doi.org/10.1002/asia.201301670.

(90) Zagidullin, A. A.; Bezkishko, I. A.; Miluykov, V. A.; Sinyashin, O. G. Phospholes - Development and Recent Advances. *Mendeleev Commun.* **2013**, *23* (3), 117–130. https://doi.org/10.1016/j.mencom.2013.05.001.

(91) Matano, Y.; Imahori, H. Design and Synthesis of Phosphole-Based π Systems for Novel Organic Materials. *Org. Biomol. Chem.* **2009**, *7* (7), 1258–1271. https://doi.org/10.1039/b819255n.

(92) Baumgartner, T.; Réau, R. Organophosphorus π-Conjugated Materials. *Chemical Reviews*. American Chemical Society November 2006, pp 4681–4727. https://doi.org/10.1021/cr040179m.

(93) Swamy P, C. A.; Priyanka, R. N.; Mukherjee, S.; Thilagar, P. Panchromatic Borane-Aza-BODIPY Conjugate: Synthesis, Intriguing Optical Properties, and Selective Fluorescent Sensing of Fluoride Anions. *Eur. J. Inorg. Chem.* **2015**, *2015* (13), 2338–2344. https://doi.org/10.1002/ejic.201500089.

(94) Affandi, S.; Green, R. L.; Hsieh, B. T.; Holt, M. S.; Nelson, J. H.; Alyea, E. C. Improved Syntheses of Tetraphenylphosphonium Bromide and 1-Phenyldibenzophosphole. *Synth. React. Inorg. Met. Chem.* **1987**, *17* (3), 307–318. https://doi.org/10.1080/00945718708059436.

(95) Wilkinson, G.; Gillard, R. D.; McCleverty, J. A. *Comprehensive Coordination Chemistry : The Synthesis, Reactions, Properties & Applications of Coordination Compounds*; Pergamon Press, 1987.

(96) Marcoux, D.; Charette, A. B. Nickel-Catalyzed Synthesis of Phosphonium Salts from Aryl Halides and Triphenylphosphine. *Adv. Synth. Catal.* **2008**, *350* (18), 2967–2974. https://doi.org/10.1002/adsc.200800542.

(97) Grim, S. O.; McFarlane, W.; Davidoff, E. F.; Marks, T. J. Phosphorus-31 Chemical Shifts of Quaternary Phosphonium Salts. *Journal of Physical Chemistry*. February 1966, pp 581–584. https://doi.org/10.1021/j100874a502.

(98) Zhao, X.; Liu, X.; Zhu, Y.; Lu, M. Palladium Nanoparticles Embedded in Improved Mesoporous Silica: A PH-Triggered Phase Transfer Catalyst for Sonogashira Reaction. *Appl. Organomet. Chem.* **2015**, *29* (10), 674–677. https://doi.org/10.1002/aoc.3349.

(99) Srinivasa Rao, P.; Gupta, A.; Bhosale, S. V.; Bilic, A.; Xiang, W.; Evans, R. A.; Bhosale, S. V. Donor–Acceptor–Acceptor-Based Non-Fullerene Acceptors Comprising Terminal Chromen-2-One Functionality for Efficient Bulk-Heterojunction Devices. *Dye. Pigment.* **2017**, *146*, 502–511. https://doi.org/10.1016/j.dyepig.2017.07.047.

(100) Zhang, S.; Zhang, Z.; Cao, R. Two- and Three-Dimensional Silver Acetylide Frameworks with

High-Nuclearity Silver Cluster Building Blocks Assembled Using a Bifunctional (4-Ethynylphenyl)Diphenyl Phosphine Ligand. *Inorganica Chim. Acta* **2017**, *461*, 57–63. https://doi.org/10.1016/j.ica.2017.01.030.

(101) Ha-Thi, M. H.; Souchon, V.; Hamdi, A.; Métivier, R.; Alain, V.; Nakatani, K.; Lacroix, P. G.; Genêt, J. P.; Michelet, V.; Leray, I. Synthesis of Novel Rod-Shaped and Star-Shaped Fluorescent Phosphane Oxides-Nonlinear Optical Properties and Photophysical Properties. *Chem. - A Eur. J.* **2006**, *12* (35), 9056–9065. https://doi.org/10.1002/chem.200600464.

(102) Peng, P.; Lu, Q.; Peng, L.; Liu, C.; Wang, G.; Lei, A. *Supporting Information Dioxygen-Induced Oxidative Activation of P-H Bond: Radical Oxyphosphorylation of Alkenes and Alkynes toward β-Oxy Phosphonates*; 2016.

(103) Huang, W.; Zhong, C.-H. Metal-Free Synthesis of Aryltriphenylphosphonium Bromides by the Reaction of Triphenylphosphine with Aryl Bromides in Refluxing Phenol. *ACS Omega* **2019**, *4* (4), 6690–6696. https://doi.org/10.1021/acsomega.9b00568.

(104) Tsipis, A. C. Exploring the Forces That Control the P-C Bond Length in Phosphamides and Their Complexes: The Key Role of Hyperconjugation. *Organometallics* **2006**, *25* (11), 2774–2781. https://doi.org/10.1021/om0600137.

(105) Misra, R.; Bhattacharyya, S. P. Intramolecular Charge Transfer : Theory and Applications.; © 2018 Wiley-VCH Verlag GmbH & Co. KGaA, 2018; pp 1–65.

(106) Kwok, W. M.; Ma, C.; George, M. W.; Grills, D. C.; Matousek, P.; Parker, A. W.; Phillips, D.; Toner, W. T.; Towrie, M. Solvent Effects on the Charge Transfer Excited States of 4-Dimethylaminobenzonitrile (DMABN) and 4-Dimethylamino-3,5-Dimethylbenzonitrile (TMABN) Studied by Time-Resolved Infrared Spectroscopy: A Direct Observation of Hydrogen Bonding Interactions. *Photochem. Photobiol. Sci.* **2007**, *6* (9), 987–994. https://doi.org/10.1039/b708414e.

(107) Haidekker, M. A.; Brady, T. P.; Lichlyter, D.; Theodorakis, E. A. Effects of Solvent Polarity and Solvent Viscosity on the Fluorescent Properties of Molecular Rotors and Related Probes. *Bioorg. Chem.* **2005**, *33* (6), 415–425. https://doi.org/10.1016/j.bioorg.2005.07.005.

(108) Stsiapura, V. I.; Maskevich, A. A.; Kuzmitsky, V. A.; Turoverov, K. K.; Kuznetsova, I. M. Computational Study of Thioflavin T Torsional Relaxation in the Excited State. *J. Phys. Chem. A* **2007**, *111* (22), 4829–4835. https://doi.org/10.1021/jp070590o.

(109) Lissau, H.; Frisenda, R.; Olsen, S. T.; Jevric, M.; Parker, C. R.; Kadziola, A.; Hansen, T.; Van Der Zant, H. S. J.; Brøndsted Nielsen, M.; Mikkelsen, K. V. Tracking Molecular Resonance Forms of Donor-Acceptor Push-Pull Molecules by Single-Molecule Conductance Experiments. *Nat. Commun.* **2015**, *6*. https://doi.org/10.1038/ncomms10233.

(110) Xue, Y.; Mou, J.; Liu, Y.; Gong, X.; Yang, Y.; An, L. An Ab Initio Simulation of the UV/Visible Spectra of Substituted Chalcones. *Cent. Eur. J. Chem.* **2010**, *8* (4), 928–936. https://doi.org/10.2478/s11532-010-0058-3.

(111) Kuno, N.; Mizutani, T. Influence of Synthetic and Natural Food Dyes on Activities of CYP2A6, UGT1A6, and UGT2B7. *J. Toxicol. Environ. Heal. Part A* **2005**, *68* (16), 1431–1444. https://doi.org/10.1080/15287390590956588.

(112) Kim, S.-Y.; Cho, Y.-J.; Lee, A.-R.; Son, H.; Han, W.-S.; Cho, D. W.; Kang, S. O. Influence of π-Conjugation Structural Changes on Intramolecular Charge Transfer and Photoinduced Electron Transfer in Donor–π–Acceptor Dyads. *Phys. Chem. Chem. Phys.* **2017**, *19* (1), 426–435. https://doi.org/10.1039/c6cp06566j.

(113) Shulov, I.; Oncul, S.; Reisch, A.; Arntz, Y.; Collot, M.; Mely, Y.; Klymchenko, A. S. Fluorinated Counterion-Enhanced Emission of Rhodamine Aggregates: Ultrabright Nanoparticles for Bioimaging and Light-Harvesting. *Nanoscale* **2015**, *7* (43), 18198–18210. https://doi.org/10.1039/c5nr04955e.

(114) Komarova, K. G.; Sakipov, S. N.; Plotnikov, V. G.; Alfimov, M. V. Luminescent Properties of Chalcone and Its Aminoderivatives. *J. Lumin.* **2015**, *164*, 57–63. https://doi.org/10.1016/j.jlumin.2015.03.021.

(115) Santhosh, K.; Grandhi, G. K.; Ghosh, S.; Samanta, A. A Fluorescence Study of the Solute-Solvent Interactions of Aminochalcones in a Room-Temperature Ionic Liquid. *Pure Appl. Chem.* **2013**, *85* (7), 1451–1463. https://doi.org/10.1351/PAC-CON-12-10-28.

(116) Schade, A.; Menzel, R.; Görls, H.; Spange, S.; Beckert, R. Negative Solvatochromism of an Anionic Thiazole-Based Dye. *Asian J. Org. Chem.* **2013**, *2* (6), 498–503. https://doi.org/10.1002/ajoc.201300085.

(117) Zhang, S.; Zhang, Z.; Cao, R. Two- and Three-Dimensional Silver Acetylide Frameworks with High-Nuclearity Silver Cluster Building Blocks Assembled Using a Bifunctional (4-Ethynylphenyl)Diphenyl Phosphine Ligand. *Inorganica Chim. Acta* **2017**, *461*, 57–63. https://doi.org/10.1016/j.ica.2017.01.030.